

National Aeronautics and Space Administration
Langley Research Center
Hampton, Virginia 23681-2199

Cloud – Aerosol LIDAR and Infrared Pathfinder Satellite Observations (CALIPSO)

Data Description and Quality Summary

Imaging Infrared Radiometer Level 2 Track Data

Data Description and Quality Summary
Imaging Infrared Radiometer Level 2 Track Data

Primary Authors

Anne Garnier

Analytical Mechanics Associates (AMA)
21 Enterprise Parkway, Hampton, Virginia 23666

Jacques Pelon

LATMOS/IPSL, Université Pierre et Marie Curie
75252 Paris Cedex 5 (France)

Nicolas Pascal

AERIS/ICARE Data and Services Center
Université de Lille
59650 Villeneuve d'Ascq (France)

Mark Vaughan, Michael Pitts, Charles Trepte, David Winker, Brian Getzewich, Jason Tackett

NASA Langley Research Center
Hampton, Virginia 23681-2199

Jayanta Kar, Kam-Pui Lee

Analytical Mechanics Associates (AMA)
21 Enterprise Parkway, Hampton, Virginia 23666

Timothy Murray, Sharon Rodier

ADNET Systems, Inc.
6720B Rockledge Drive, Suite #504, Bethesda, Maryland 20817

Robert Ryan

Coherent Applications, Inc. – Psionic LLC
1100 Exploration Way, Hampton, Virginia 23666

January 30, 2026

CALIPSO IIR Level 2 Track Data Description Document

Version 5.00

Data Version: 5.00
Data Release Date: October 01, 2025
Data Date Range: June 13, 2006 to June 30, 2023

Introduction

The primary geophysical variables reported in the IIR Level 2 track data products at 1-km pixel resolution are the measured brightness temperatures under the lidar track in the three IIR channels (8.65, 10.60 and 12.05 μm), a scene classification, effective emissivity in each IIR channel and microphysical properties. For consistency with the CALIOP products, the products are partitioned into daytime and nighttime granules corresponding to approximately one-half orbit each.

The IIR Level 2 track algorithm, described in Garnier et al. ([2021a](#), [2021b](#)), takes full advantage of the co-located characterization of the atmosphere provided by CALIOP. It is applied to suitable types of scenes classified using the Version 5.00 (V5) CALIOP 5-km Cloud and Aerosol 5-km layer products. The retrievals are applied to the so-called *upper level* which includes either one single semi-transparent or opaque layer, or several semi-transparent layers. Emissivity retrievals require a correction for the contribution from the “background”. When the lowermost of at least two layers in the column is opaque to CALIOP, the background reference is from this opaque layer, which is called *lower level*. Otherwise, the reference is from the Earth surface. *Upper and lower level* properties inferred from CALIOP are also provided.

Microphysical retrievals use the concept of microphysical index (β_{eff}) ([Parol et al., 1991](#)) applied to the IIR pairs of channels (12.05, 10.6) and (12.05, 8.65), with $\beta_{\text{eff}12/10}$ and $\beta_{\text{eff}12/08}$ defined as the 12.05-to-10.6 and 12.05-to-08.65 ratios of the effective absorption optical depths, respectively.

In the standard algorithm, the microphysical indices are interpreted in terms of effective diameter, D_e , by using Look-Up Tables (LUTs) built using the Fast Discrete Ordinate Method (FASDOM) radiative transfer model ([Dubuisson et al., 2005, 2008](#)) for several particle models with a gamma particle size distribution. For ice clouds, the standard algorithm uses two ice crystal models, namely severely rough “single hexagonal column” and “8-element column aggregate” ([Yang et al., 2013](#); [Bi and Yang, 2017](#)), and D_e is retrieved using the ice crystal model that provides the best agreement with the observations in terms of relationship between $\beta_{\text{eff}12/10}$ and $\beta_{\text{eff}12/08}$. For liquid water clouds, the algorithm uses dedicated LUTs derived from Mie calculations.

For this V5 data release, the algorithm uses the temperature and extinction profiles reported in the V5 CALIOP cloud profile products to improve the radiative temperature estimate and to produce a new series of retrievals when the *upper level* is composed of semi-transparent ice clouds (new SDS names starting with “Cirrus”). New optical and microphysical properties including (but not limited to) layer ice number concentration, D_e and ice water content are retrieved using new analytical functions relating $\beta_{\text{eff}12/10}$ and various microphysical quantities derived from in situ measurements at tropical and mid-latitudes performed during the TC4, ATTREX, POSIDON, and SPARTICUS field experiments ([Mitchell et al., 2025](#)).

Table of Contents

Introduction	3
Additional documentation	8
Glossary and Acronym Dictionary	9
Data Product Descriptions	10
Latitude	10
Longitude	10
LIDAR_Shot_Time.....	10
LIDAR_Profile_ID.....	10
IIR_Image_Time_12_05	10
Brightness_Temperature_08_65	11
Brightness_Temperature_12_05	11
Brightness_Temperature_10_60	11
Type_of_Scene.....	11
Was_Cleared_Flag_1km.....	13
Multi_Layer_Flag.....	14
Effective_Emissivity_08_65.....	14
Effective_Emissivity_12_05.....	14
Effective_Emissivity_10_60.....	14
Effective_Emissivity_Uncertainty_08_65	15
Effective_Emissivity_Uncertainty_12_05	15
Effective_Emissivity_Uncertainty_10_60	15
Effective_Emissivity_Uncertainty_Terms_08_65	15
Effective_Emissivity_Uncertainty_Terms_12_05	15
Effective_Emissivity_Uncertainty_Terms_10_60	15
Particle_Shape_Index.....	15
Particle_Shape_Index_Confidence	16
Effective_Particle_Size	16
Effective_Particle_Size_Uncertainty	16
Ice_Liquid_Water_Path.....	16
Ice_Liquid_Water_Path_Confidence	17
Reference_Brightness_Temperature	17
Blackbody_Brightness_Temperature.....	17
Computed_Brightness_Temperature_Surface	17
Optical_Depth_12_05.....	18
Optical_Depth_12_05_Uncertainty.....	18
Optical_Depth_0532_Upper_Level.....	18

Depolarization_Upper_Level	18
Integrated_Backscatter_Upper_Level	19
Layer_Top_Height_Upper_Level.....	19
Centroid_IAB_0532_Upper_Level.....	19
Layer_Bottom_Height_Upper_Level	19
Layer_Top_Temperature_Upper_Level.....	20
Temperature_Centroid_IAB_0532_Upper_Level	20
Layer_Bottom_Temperature_Upper_Level.....	20
Layer_Top_Pressure_Upper_Level	20
Pressure_Centroid_IAB_0532_Upper_Level.....	20
Layer_Bottom_Pressure_Upper_Level	20
Ice_Water_Flag_Upper_Level.....	21
Ice_Water_Flag_QA_Upper_Level.....	21
Ice_Water_Path_CALIOP_Upper_Level	22
Optical_Depth_0532_Lower_Level.....	22
Depolarization_Lower_Level.....	22
Integrated_Backscatter_Lower_Level	22
Layer_Top_Height_Lower_Level.....	22
Centroid_IAB_0532_Lower_Level.....	23
Layer_Bottom_Height_Lower_Level.....	23
Layer_Top_Temperature_Lower_Level	23
Temperature_Centroid_IAB_0532_Lower_Level	23
Layer_Bottom_Temperature_Lower_Level	23
Layer_Top_Pressure_Lower_Level	24
Pressure_Centroid_IAB_0532_Lower_Level.....	24
Layer_Bottom_Pressure_Lower_Level	24
Ice_Water_Flag_Lower_Level.....	24
Ice_Water_Flag_QA_Lower_Level	25
Surface_Emissivity_08_65	25
Surface_Emissivity_12_05	25
Surface_Emissivity_10_60	25
IGBP_Surface_Type.....	26
Snow_Ice_Surface_Type	26
Surface_532_Integrated_Depolarization_Ratio	27
TGeotype.....	27
Initial_Surface_Temperature	27

Surface_Temperature	28
IIR_Data_Quality_Flag.....	28
Equalization_Flag	28
LIDAR_Data_Quality_Flag	29
Surrounding_Obs_Quality_Flag	29
High_Cloud_vs_Background_Flag.....	30
Computed_vs_Observed_Flag	31
Regional_Background_Std_Dev_Flag	31
Microphysics	31
Dust_Stratospheric_Aerosol_Flag.....	32
Dust_Stratospheric_Aerosol_Flag_QA.....	32
Reflectance.....	33
Integrated_Water_Vapor_Path	33
Radiative_Temperature_Upper_Level.....	33
Radiative_Height_Upper_Level	33
Radiative_Pressure_Upper_Level.....	33
Cloud_Optical_Depth.....	34
Cloud_Optical_Depth_Uncertainty.....	34
Cirrus_IIR_Thickness	34
Cirrus_Number_Concentration.....	34
Cirrus_Number_Concentration_Uncertainty.....	34
Cirrus_IIR_Extinction.....	35
Cirrus_IIR_Extinction_Uncertainty.....	35
Cirrus_Optical_Depth.....	35
Cirrus_Optical_Depth_Uncertainty.....	35
Cirrus_Effective_Diameter.....	35
Cirrus_Effective_Diameter_Uncertainty.....	35
Cirrus_Ice_Water_Content	36
Cirrus_Ice_Water_Content_Uncertainty	36
Cirrus_Ice_Water_Path.....	36
Cirrus_Ice_Water_Content_Uncertainty	36
Cirrus_Volume_Radius.....	36
Cirrus_Volume_Radius_Uncertainty.....	37
Low_Energy_Mitigation_Column_QC_Flag	37
Metadata Parameter Descriptions.....	37
Product_ID	37

Date_Time_at_Granule_Start	38
Date_Time_at_Granule_End.....	38
Date_Time_of_Production.....	38
Initial_IIR_Scan_Center_Latitude.....	38
Initial_IIR_Scan_Center_Longitude.....	38
Ending_IIR_Scan_Center_Latitude.....	38
Ending_IIR_Scan_Center_Longitude.....	38
Path_Number_at_Granule_Start.....	38
Path_Number_at_Granule_Stop	38
Path_Number_Change_Time.....	38
Number_of_IIR_Records_in_File	39
Number_of_Valid_08_65_Pixels.....	39
Number_of_Valid_12_05_Pixels.....	39
Number_of_Valid_10_60_Pixels.....	39
Number_of_Invalid_08_65_Pixels	39
Number_of_Invalid_12_05_Pixels	39
Number_of_Invalid_10_60_Pixels.....	39
Number_of_Rejected_08_65_Pixels.....	39
Number_of_Rejected_12_05_Pixels.....	39
Number_of_Rejected_10_60_Pixels.....	39
Number_of_Rejected_08_65_Pixels_Location.....	39
Number_of_Rejected_12_05_Pixels_Location.....	39
Number_of_Rejected_10_60_Pixels_Location.....	39
Number_of_Rejected_08_65_Pixels_Radiance.....	40
Number_of_Rejected_12_05_Pixels_Radiance.....	40
Number_of_Rejected_10_60_Pixels_Radiance.....	40
Mean_08_65_Radiance_All	40
Mean_12_05_Radiance_All	40
Mean_10_60_Radiance_All	40
Mean_08_65_Radiance_Selected_Cases	40
Mean_12_05_Radiance_Selected_Cases	40
Mean_10_60_Radiance_Selected_Cases	40
Mean_08_65_Brightness_Temp_All.....	40
Mean_12_05_Brightness_Temp_All.....	40
Mean_10_60_Brightness_Temp_All.....	40
Mean_08_65_Brightness_Temp_Selected_Cases.....	40

Mean_12_05_Brightness_Temp_Selected_Cases	40
Mean_10_60_Brightness_Temp_Selected_Cases	40
Number_of_Valid_LIDAR_Pixels	41
Number_of_Invalid_LIDAR_Pixels.....	41
Number_of_Rejected_LIDAR_Pixels	41
Number_of_Selected_Cloud_Cases.....	41
Percent_of_Selected_Cloud_Cases	41
Number_of_Selected_Aerosol_Cases.....	41
Percent_of_Selected_Aerosol_Cases	41
Number_of_Identified_Pixels_Clear_Sky	41
Percent_of_Identified_Pixels_Clear_Sky	41
Mean_Altitude_High_Cloud.....	41
GEOS_Version	41
Data Release Information	41
Data Quality Information	42
Data Quality Statement for the release of the CALIPSO IIR Level 2 Product Version 5.00.....	42
Data Quality Statement for the release of the CALIPSO IIR Level 2 Product Version 4.51.....	46
Data Quality Statement for the release of the CALIPSO IIR Level 2 Product Version 4.21.....	46
Data Quality Statement for the release of the CALIPSO IIR Level 2 Product Version 4.20.....	47
Data Quality Statement for the release of the CALIPSO IIR Level 2 Product Version 3.46.....	50
Data Quality Statement for the release of the CALIPSO IIR Level 2 Product Version 3.45.....	50
Data Quality Statement for the release of the CALIPSO IIR Level 2 Product Version 3.40.....	50
Data Quality Statement for the release of the CALIPSO IIR Level 2 Product Version 3.30.....	50
Data Quality Statement for the release of the CALIPSO IIR Level 2 Product Version 3.02.....	51
Data Quality Statement for the release of the CALIPSO IIR Level 2 Product Version 3.01.....	51
Data Quality Statement for the release of the CALIPSO IIR Level 2 Product Version 2.20.....	51
Data Quality Statement for the release of the CALIPSO IIR Level 2 Product Version 2.01.....	51
References.....	52

Additional documentation

Project Documentation

- CALIPSO Data Management Team: CALIPSO Data Products Catalog, PC-SCI-503, Release 5.00.
- Pelon, J., A. Garnier, O. Chomette, M. Viollier, P. Dubuisson, V. Giraud, F. Parol, S. A. Ackerman, D. P. Kratz, Y. Hu, and M. R. Platt, CALIPSO IIR Algorithm Theoretical Basis Document, Level 2 data products, PC-SCI-204, <https://ntrs.nasa.gov/citations/20250008391>.

Peer-Reviewed Algorithm Papers

- Dubuisson, P., V. Giraud, O. Chomette, H. Chepfer, and J. Pelon, 2005: Fast radiative transfer modeling for infrared imaging radiometry. *J. Quant. Spectrosc. Radiat. Transfer*, **95**, 201–220, <https://doi.org/10.1016/j.jqsrt.2004.09.034>.
- Dubuisson, P., V. Giraud, J. Pelon, B. Cadet, and P. Yang, 2008: Sensitivity of Thermal Infrared Radiation at the Top of the Atmosphere and the Surface to Ice Cloud Microphysics, *J. Appl. Meteor. Climatol.*, **47**, 2545–2560, <https://doi.org/10.1175/2008JAMC1805.1>.
- Garnier, A., J. Pelon, P. Dubuisson, M. Faivre, O. Chomette, N. Pascal and D. P. Kratz, 2012: Retrieval of cloud properties using CALIPSO Imaging Infrared Radiometer. Part I: effective emissivity and optical depth, *J. Appl. Meteor. Climatol.*, **51**, 1407–1425, <https://doi.org/10.1175/JAMC-D-11-0220.1>.
- Garnier, A., J. Pelon, P. Dubuisson, P. Yang, M. Faivre, O. Chomette, N. Pascal, P. Lucker and T. Murray, 2013: Retrieval of cloud properties using CALIPSO Imaging Infrared Radiometer. Part II: effective diameter and ice water path, *J. Appl. Meteor. Climatol.*, **52**, 2582–2599, <https://doi.org/10.1175/JAMC-D-12-0328.1>.
- Mitchell, D. L., A. Garnier, J. Pelon and E. Erfani, 2018: CALIPSO (IIR-CALIOP) Retrievals of Cirrus Cloud Ice Particle Concentrations, *Atmos. Chem. Phys.*, **18**, 17325–17354, <https://doi.org/10.5194/acp-18-17325-2018>.
- Garnier, A., J. Pelon, N. Pascal, M. A. Vaughan, P. Dubuisson, P. Yang and D. L. Mitchell, 2021a: Version 4 CALIPSO IIR ice and liquid water cloud microphysical properties, Part I: the retrieval algorithms, *Atmos. Meas. Tech.*, **14**, 3253–3276, <https://doi.org/10.5194/amt-14-3253-2021>.
- Garnier, A., J. Pelon, N. Pascal, M. A. Vaughan, P. Dubuisson, P. Yang and D. L. Mitchell, 2021b: Version 4 CALIPSO IIR ice and liquid water cloud microphysical properties, Part II: results over oceans, *Atmos. Meas. Tech.*, **14**, 3277–3299, <https://doi.org/10.5194/amt-14-3277-2021>.
- Mitchell, D. L., A. Garnier, and S. Woods, 2025: Advances in CALIPSO (IIR) cirrus cloud property retrievals – Part 1: Methods and testing, *Atmos. Chem. Phys.*, **25**, 14071–14098, <https://doi.org/10.5194/acp-25-14071-2025>.

Glossary and Acronym Dictionary

Term	Meaning
AFWA	U.S. Air Force Weather Agency
ATTREX	Airborne Tropical Tropopause Experiment
β_{eff}	microphysical index
CALIOP	Cloud-Aerosol Lidar with Orthogonal Polarization
CALIPSO	Cloud-Aerosol Lidar and Infrared Pathfinder Satellite Observation
D_e	effective diameter
GEOS	Goddard Earth Observing System
granule	continuous data segment in which all measurements were acquired while the lidar was configured for daytime data acquisition only or nighttime data acquisition only; each granule spans approximately one half of a full orbit, with daytime granules being slightly larger/longer than nighttime granules
HDF	Hierarchical Data Format
HOI	Horizontally Oriented Ice
IAB	Integrated Attenuated Backscatter
IGPB	International Geosphere–Biosphere Programme
IIR	Imaging Infrared Radiometer
LEM	Low Energy Mitigation
LUT	Look-Up Table

MERRA-2	Modern-Era Retrospective Analysis for Research and Applications, Version 2
N/A	Not Applicable
POSIDON	Pacific Oxidants Sulfur Ice and DehydratiON
QA	quality assurance/quality control
ROI	Randomly Oriented Ice
SDS	Scientific Data Set
SPARTICUS	Small Particles In Cirrus
TAI	International Atomic Time
TC4	Tropical Composition, Cloud and Climate Coupling Experiment
UTC	Coordinated Universal Time
WRS	Worldwide Reference System

Data Product Descriptions

Latitude

Units: degrees_north

Format: Float_32

Valid Range: -90.0, 90.0

Fill Value: -9999.0

Description: Geodetic latitude at the center of the pixel, duplicate of the Latitude parameter in the Level 1B IIR product.

Longitude

Units: degrees_east

Format: Float_32

Valid Range: -180.0, 180.0

Fill Value: -9999.0

Description: Longitude at the center of the pixel, duplicate of the Longitude parameter in the Level 1B IIR product.

LIDAR_Shot_Time

Units: TAI seconds

Format: Float_64

Valid Range: 4.204E8, 9.623E8

Fill Value: -9999.0

Description: Duplicate of the Lidar_Shot_Time in the Level 1B IIR product. International Atomic Time (TAI) in elapsed seconds from January 1, 1993.

LIDAR_Profile_ID

Units: NoUnits

Format: Int_32

Valid Range: 1,228630

Fill Value: -9999

Description: Identification number of the CALIOP single shot profile collocated with the center of the IIR pixel.

IIR_Image_Time_12_05

Units: TAI seconds

Format: Float_64

Valid Range: 4.204E8, 9.623E8

Fill Value: -9999.0

Description: Duplicate of the Image_Time_12.05 in the Level 1B IIR product. International Atomic Time (TAI) in elapsed seconds from January 1, 1993.

Brightness_Temperature_08_65

Brightness_Temperature_12_05

Brightness_Temperature_10_60

Units: K

Format: Float_32

Valid Range: 0.0, 400.0

Fill Value: -9999.0

Description: Brightness temperature of IIR channels 8.65, 12.05 and 10.6 calculated from the corresponding IIR Level 1 calibrated radiance using the equation and the coefficients given in Sect. 2.4 of [Garnier et al. \(2018\)](#).

Type_of_Scene

Units: NoUnits

Format: Int_8

Valid Range: 0, 99

Fill Value: -99

Description: Scene classification derived from the CALIOP Level 2 Cloud and Aerosol 5-km layer data products, designed to select the scenes to be further analyzed in term of effective emissivity and in the meantime to be possibly compared with existing clouds classifications. Only layers identified with a 5 or 20-km horizontal resolution are used in the analysis, except for CLEAR SKY and AEROSOLS ONLY scenes 51 to 56 which do not contain clouds at any resolution. The scenes are first organized according to the background reference type of scene (4th column in the table below), which can be either the surface (low non-depolarizing semi-transparent aerosol layers may be accepted) or an opaque layer (*lower level*). For each category, one to several semi-transparent (ST) layers can be considered as the *upper level* to compute the effective emissivity (3rd column in the table). Layers are high when their centroid altitude is above 7 km and are low otherwise. Clear sky scenes (10) and scenes containing only aerosol layers (Types 51 to 57 and 64) are classified as such if Was_Cleared_Flag_1km = 0. If Was_Cleared_Flag_1km > 0, they are assigned new type of scenes (50 and 91 to 98, see "OTHERS") and no IIR retrievals are attempted. A low altitude ST cloud layer (Type 24) is re-classified into Type 59 if the maximum attenuated backscatter and the maximum volume depolarization ratio in the layer are smaller than 0.02 sr⁻¹ and 6% respectively, as a possible indicator of the presence of aerosols. Scenes containing one single high ST cloud or one single high ST aerosol layer over a high opaque cloud are classified as types 81 or 85 if the distance between the centroid altitudes of the ST and opaque layers is smaller than 1 km, and they are processed as a single layer.

The scenes with lidar data that do not match the classification are reported as Type 99. For this version 5.00 data release, the IIR pixels in 5-km columns that are rejected by the CALIOP Low Energy Mitigation algorithm (LEM, [Tackett et al., 2025](#)) fall into that category.

The scenes with no co-located lidar data are assigned a fill value.

Table 1: Interpretation of Type of Scene

Value	Description	Number of Layers in Upper Level	Reference Type of Scene
	CLEAR SKY, Was_Cleared_Flags_1km = 0		
10	Clear sky (no aerosol layer)	N/A	N/A
	AEROSOLS ONLY, Was_Cleared_Flags_1km = 0		
51	1 to 4 high ST aerosol layer(s)	1 to 4	10
52	1 to 4 low ST aerosol layer(s), all layers have mean volume depolarization ratio < 6%	1 to 4	10
53	1 to 4 low ST aerosol layer(s), at least one layer has mean volume depolarization ratio > 6%	1 to 4	10
54	1 to 4 high ST aerosol layer(s) and 1 to 3 low ST aerosol layer(s)	2 to 5	10
55	1 high opaque layer	1	10
56	1 low opaque aerosol layer	1	10
64	1 to 4 high ST aerosol layer(s)/ 1 low opaque aerosol layer	1 to 4	56
57	Any other aerosol layer(s) only	1 to 8	10
	CLOUDS		
20	Low opaque cloud, no aerosol, maximum volume depolarization ratio >40%	1	10 (or 52 backup)
70	Low opaque cloud, no aerosol, maximum volume depolarization ratio < 40%	1	10 (or 52 backup)
40	High opaque cloud, no aerosol, maximum volume depolarization ratio >40%	1	10 (or 52 backup)
80	High opaque cloud, no aerosol, maximum volume depolarization ratio < 40%	1	10 (or 52 backup)
81	1 high ST cloud and 1 high opaque cloud Centroid altitudes difference < 1 km	1	10 (or 52 backup)
85	1 high ST aerosol and 1 high opaque cloud Centroid altitudes difference < 1 km	1	10 (or 52 backup)
21	1 high ST cloud only (no aerosol)	1	10
22	2 high ST clouds, no high ST aerosol layer, up to 4 low ST aerosol layers	2	10 (or 52 backup)
23	1 high ST cloud and 1 low ST cloud, no high ST aerosol layer, up to 4 low ST aerosol layers	2	10 (or 52 backup)
24	1 low ST cloud, no high ST aerosol layer, maximum 532-nm attenuated_backscatter > 0.02 sr ⁻¹ or maximum volume depolarization ratio > 6%	1	10 (or 52 backup)
59	1 low ST cloud, no high ST aerosol layer, maximum 532-nm attenuated_backscatter < 0.02 sr ⁻¹ and maximum volume depolarization ratio < 6%	1	10 (or 52 backup)
25	2 low ST clouds only (no aerosol layer)	2	10 (or 52 backup)
26	3 high ST clouds	3	10 (or 52 backup)
27	2 high ST clouds and 1 low ST cloud	3	10 (or 52 backup)
67	3-4 high ST clouds and 1 low ST cloud	4 or 5	10 (or 52 backup)
28	1 high ST cloud and 2 low ST clouds	3	10 (or 52 backup)
68	2-3 high ST clouds and 2 low ST clouds or 3 high ST clouds and 3 low ST clouds	4 to 6	10 (or 52 backup)
29	3 to 7 low ST clouds only (no aerosols)	3 to 7	10
31	1 high ST cloud / 1 low opaque cloud, no high ST aerosol layer, up to 4 low ST aerosol layers	1	20

Value	Description	Number of Layers in Upper Level	Reference Type of Scene
32	2 to 6 high ST cloud/ 1 opaque cloud	2 to 6	20
62	3 to 6 ST cloud (at least 1 high ST and 1 low ST)/ 1 opaque cloud	3 to 6	20
33	1 high ST cloud and 1 low ST cloud / 1 opaque cloud	2	20
34	1 low ST cloud/ 1 opaque cloud	1	20
39	2 to 4 low ST clouds/ 1 low opaque cloud	2 to 4	20
41	1 high ST cloud/ 1 high opaque cloud Centroid altitudes difference > 1 km	1	40
42	2 high ST cloud/ 1 high opaque cloud	2	40
	MIXED AEROSOLS/CLOUDS		
30	1 high ST cloud / 1 to 4 low ST aerosol layers	1	52
66	1 high ST aerosol layer above 1 high ST cloud and 1 low ST cloud	3	10 (or 52 backup)
63	1 to 4 low aerosol layers above 1 low ST cloud	2 to 5	10 (or 52 backup)
35	1 to 4 high ST aerosol layers / 1 low opaque cloud	1 to 4	20
36	1 to 4 low ST aerosol layers / 1 low opaque cloud	1 to 4	20
37	1 high ST cloud / 1 low opaque aerosol layer	1	56
38	1 low ST cloud / 1 low opaque aerosol layer	1	56
65	1 to 4 high ST aerosol layers / 1 high opaque cloud If 1 high ST aerosol layer, centroid altitudes difference must be > 1 km	1 to 4	40
	OTHERS		
50	Clear sky (no aerosol layer) Was_Cleared_Flag_1km > 0	N/A	N/A
91	1 to 4 high ST aerosol layer(s) Was_Cleared_Flag_1km > 0	N/A	N/A
92	1 to 4 low ST aerosol layer(s), all layers have mean volume depolarization ratio < 6% Was_Cleared_Flag_1km > 0	N/A	N/A
93	1 to 4 low ST aerosol layer(s), at least one layer has mean volume depolarization ratio > 6% Was_Cleared_Flag_1km > 0	N/A	N/A
94	1 to 4 high ST aerosol layer(s) and 1 to 3 low ST aerosol layer(s) Was_Cleared_Flag_1km > 0	N/A	N/A
95	1 high opaque aerosol layer Was_Cleared_Flag_1km > 0	N/A	N/A
96	1 low opaque aerosol layer Was_Cleared_Flag_1km > 0	N/A	N/A
97	Any other aerosol layers only Was_Cleared_Flag_1km > 0	N/A	N/A
98	1 to 4 high ST aerosol layer(s)/ 1 low opaque aerosol layer Was_Cleared_Flag_1km > 0	N/A	N/A
99	No classification or 5-km column rejected by the CALIOP LEM algorithm	N/A	N/A

Was_Cleared_Flag_1km

Units: NoUnits

Format: Int_8

Valid Range: 0, 30

Fill Value: -99

Description: The units indicate the number of CALIOP single shot clouds in the atmospheric column seen by the 1 km IIR pixel that were cleared from the CALIOP 5 km layer products (cf CALIOP’s “ssWas_Cleared” SDS). The tens indicate the number of single shot profiles rejected by the CALIOP Low Energy Mitigation (LEM) algorithm.

Table 2: Interpretation of Was Cleared Flag 1 km

		<i>Number of cleared shots in 1-km IIR pixel</i>			
		<i>0</i>	<i>1</i>	<i>2</i>	<i>3</i>
<i>Number of LEM rejected single-shot profiles in 1-km IIR pixel</i>	<i>0</i>	0	1	2	3
	<i>1</i>	10	11	12	N/A
	<i>2</i>	20	21	N/A	N/A
	<i>3</i>	30	N/A	N/A	N/A

Multi_Layer_Flag

Units: NoUnits

Format: Float_32

Valid Range: -8030.0, 8030.0

Fill Value: -9999.0

Description: Provides the number of layers included in the *upper level*, as well as the difference in km between the base altitude of the uppermost layer and the top altitude of the lowermost layer. This flag takes the sign of this difference, which can be negative in case of overlapping layers. When the *upper level* contains only one layer this difference is set to 0 and the flag is set to 1000.

Table 3: Interpretation of Multi Layer Flag

Digits	Interpretation
Tens-Units_Decimal	Difference between the bottom altitude of the uppermost layer and the top altitude of the lowermost layer of the <i>upper level</i> . Multi_Layer_Flag takes the sign of this quantity. This quantity is set to zero for mono-layer cases.
Hundreds	0
Tens-thousands-and thousands	Number of layers in the <i>upper level</i> .

Effective_Emissivity_08_65

Effective_Emissivity_12_05

Effective_Emissivity_10_60

Units: NoUnits

Format: Float_32

Valid Range: 0.0, 1.0

Fill Value: -9999.0

Description: Effective emissivity for IIR channels 8.65, 12.05 and 10.6 of the *upper level* associated to Type_of_Scene. Emissivities found outside of the range 0 to 1 are considered non-physical and are due to retrieval errors.

Effective_Emissivity_Uncertainty_08_65

Effective_Emissivity_Uncertainty_12_05

Effective_Emissivity_Uncertainty_10_60

Units: NoUnits

Format: Float_32

Valid Range: 0.0, 1.0

Fill Value: -9999.0

Description: Estimated uncertainty in the effective emissivity for IIR channels 8.65, 12.05 and 10.6. For each channel, this global uncertainty is derived from the 3 terms reported in the respective Effective_Emissivity_Uncertainty_Terms_* SDSs.

Effective_Emissivity_Uncertainty_Terms_08_65

Effective_Emissivity_Uncertainty_Terms_12_05

Effective_Emissivity_Uncertainty_Terms_10_60

Units: NoUnits

Format: Float_32

Valid Range: First term: -1.0, 0.0; second and third terms: 0.0, 1.0

Fill Value: -9999.0

Description: Terms used to compute the estimated uncertainty in the effective emissivity for IIR channels 8.65, 12.05 and 10.6 (appendix A in [Garnier et al., 2021a](#)) The three records report the sensitivity of the effective emissivity to (in this order):

- an error $dT_m = 0.3$ K in the measured brightness temperature,
- an error dT_{BG} (1 K over water surface; 3 K over non-water surface) in the background reference brightness temperature,
- an error $dT_{BB} = 2$ K in the blackbody temperature.

Particle_Shape_Index

Units: NoUnits

Format: Int_8

Valid Range: 1, 9

Fill Value: -99

Description: Identifies the model that was used to retrieve the Effective_Particle_Size. If all the layers are liquid water clouds, the water model is used. If all the layers are ice clouds, the ice model is determined by minimizing the mean squared difference between the retrieved ($\beta_{\text{eff}12/10}$, $\beta_{\text{eff}12/08}$) pair of microphysical indices and the ensemble of pairs available in the ice LUTs. If at least one cloud layer has an unknown phase, or in case of multi-layer systems that include both ice and water clouds, both the ice and water models are considered in the search of the best agreement with the retrievals. If only one microphysical index could be computed (because effective emissivity at 08.65 or at 10.60 μm is negative or larger than 1), the model is guessed. Retrievals are not attempted for aerosol layers, except for stratospheric aerosol layers classified as "polar aerosol" or "volcanic ash" that may be ice clouds in case of misclassification. In these specific cases, ice models are used. This parameter is set to a fill value if none of the $\beta_{\text{eff}12/10}$ and $\beta_{\text{eff}12/08}$ microphysical indices can be computed or if no microphysical retrievals are attempted.

Table 4: Interpretation of Particle Shape Index

Value	Interpretation
1	Water
7	Severely rough 8-element column aggregate
9	Severely rough single hexagonal column

Particle_Shape_Index_Confidence

Units: NoUnits

Format: Int_8

Valid Range: 1, 4

Fill Value: -99

Description: Index that reflects the agreement between the retrieved ($\beta_{\text{eff}12/10}$, $\beta_{\text{eff}12/08}$) pair of microphysical indices and the selected model. Confidence is considered as good (1) when both diameters agree within 30% and medium (2) otherwise. When only one microphysical index can be computed, the algorithm uses a best guess model, and this index is set to 3. When at least one microphysical index is not within the expected range of values, this index is set to 4 (no confidence). A fill value indicates that none of the microphysical indices can be computed or that no microphysical retrievals are attempted.

Effective_Particle_Size

Units: μm

Format: Float_32

Valid Range: 0.0, 200.0

Fill Value: -9999.0

Description: Effective diameter D_e of the *upper level* associated to Type_of_scene. When both $\beta_{\text{eff}12/10}$ and $\beta_{\text{eff}12/08}$ microphysical indices can be retrieved, this parameter is the mean of the effective diameters $D_{e12/10}$ and $D_{e12/08}$ retrieved from the respective microphysical indices and the model identified in Particle_Shape_Index. When only one microphysical index can be computed, D_e is retrieved from this microphysical index using the best guess model. Effective_Particle_Size should not be used when the microphysical indices are not within the expected range of values, that is when Particle_Shape_Index_Confidence is equal to 4. The full set of $D_{e12/10}$ and $D_{e12/08}$ associated to each shape is provided in Microphysics.

Effective_Particle_Size_Uncertainty

Units: μm

Format: Float_32

Valid Range: 0.0, 200.0

Fill Value: -9999.0

Description: Estimated absolute uncertainty in the effective diameter reported in Effective_Particle_Size. It is inferred from the LUTs and the estimated uncertainty in the microphysical indices (see appendix A in [Garnier et al., 2021a](#)). When the microphysical indices are outside the expected range of values available in the LUTs, the uncertainty is not estimated.

Ice_Liquid_Water_Path

Units: $\text{g}/(\text{m}^2)$

Format: Float_32

Valid Range: 0.0, 1300.0

Fill Value: -9999.0

Description: Estimate of the ice water path when the *upper level* includes only ice clouds and of the liquid water path when the *upper level* includes only water clouds as reported in the Ice_Water_Flag_Upper_Level (see Section 5 of [Garnier et al., 2021a](#)).

Ice_Liquid_Water_Path_Confidence

Units: g/(m²)

Format: Float_32

Valid Range: 0.0, 1300.0

Fill Value: -9999.0

Description: Estimated absolute uncertainty in the ice or liquid water path reported in Ice_Liquid_Water_Path.

Reference_Brightness_Temperature

Units: K

Format: Int_16

Valid Range: 0, 400

Fill Value: -9999

Scale Factor: 100.0

Offset: 100.0

Scale Equation: data/scale_factor + offset

Description: This parameter contains six records. The first three records are the background reference brightness temperatures at 08.65, 10.60 and 12.05 μm , as computed using the FASRAD radiative transfer model ([Dubuisson et al., 2005](#)) and Temperature_Centroid_IAB_0532_Lower_Level if the reference is an opaque layer. The last three records are the background reference brightness temperatures used to retrieve the effective emissivity of the *upper level*. They may differ from the first three records when the reference is measured in neighboring pixels (cf High_Cloud_vs_Background) or if the opaque reference is an ice layer. This parameter is a fill value if no effective emissivity retrievals are attempted.

Blackbody_Brightness_Temperature

Units: K

Format: Int_16

Valid Range: 0, 400

Fill Value: -9999

Scale Factor: 100.0

Offset: 100.0

Scale Equation: data/scale_factor + offset

Description: This parameter contains six records. The first three records are the blackbody brightness temperatures at 08.65, 10.60 and 12.05, as computed using the FASRAD radiative transfer model ([Dubuisson et al., 2005](#)) and Temperature_Centroid_IAB_0532_Upper_Level. The last three records are the blackbody brightness temperatures used to retrieve the effective emissivity of the *upper level* and are computed using Radiative_Temperature_Upper_Level. They differ from the first three records when the *upper level* is composed of ice clouds. This parameter is a fill value if no effective emissivity retrievals are attempted.

Computed_Brightness_Temperature_Surface

Units: K

Format: Int_16

Valid Range: 0, 400

Fill Value: -9999

Scale Factor: 100.0

Offset: 100.0

Scale Equation: data/scale_factor + offset

Description: Equivalent brightness temperature of the clear sky surface radiance as computed using the FASRAD radiative transfer model ([Dubuisson et al., 2005](#)). FASRAD uses atmospheric profiles and skin temperatures from the MERRA 2 model, and surface emissivities reported in the product. This parameter is reported for all types of scenes.

Optical_Depth_12_05

Units: NoUnits

Format: Float_32

Valid Range: 0.0, 10.0

Fill Value: -9999.0

Description: Effective absorption optical depth in IIR channel 12.05 derived from the effective emissivity at 12.05 microns if the latter is found between 0 and 1 (equation 2 in [Garnier et al., 2021a](#)). Absorption optical depths larger than 10 (i.e. effective emissivity at 12.05 microns larger than 0.9999546) are not reported.

Optical_Depth_12_05_Uncertainty

Units: NoUnits

Format: Float_32

Valid Range: 0.0, 10.0

Fill Value: -9999.0

Description: Estimated absolute uncertainty in Optical_Depth_12_05 (see appendix A in [Garnier et al., 2021a](#)). Uncertainties larger than 10 are not reported.

Optical_Depth_0532_Upper_Level

Units: NoUnits

Format: Float_32

Valid Range: 0.0, 5.0

Fill Value: -9999.0

Description: Summation of the layer's optical depths at 532 nm as provided in the CALIOP lidar Level 2 Cloud and/or Aerosol layer products for the layers included in the *upper level*. This parameter is set to a fill value when no IIR retrievals are attempted.

Depolarization_Upper_Level

Units: NoUnits

Format: Float_32

Valid Range: 0.0, 1.0

Fill Value: -9999.0

Description: Integrated particulate depolarization ratio of the *upper level* derived from CALIOP observations, where the contribution of each layer of the *upper level* depends on its integrated particulate depolarization ratio, its 532 nm integrated attenuated backscatter and the 532 nm overlying two-way transmittance. For single-layer *upper levels*, Depolarization_Upper_Level is simply

Integrated_Particiulate_Depolarization_Ratio reported by CALIOP. This parameter is set to a fill value when no IIR retrievals are attempted.

Integrated_Backscatter_Upper_Level

Units: 1/sr

Format: Float_32

Valid Range: 0.0, 1.0

Fill Value: -9999.0

Description: Integrated attenuated backscatter at 532 nm of the *upper level* (IAB) derived from CALIOP observations. It is the summation of the IABs reported in the CALIOP Level 2 Cloud and/or Aerosol layer products for each layer of the *upper level*, weighted by the 532 nm two-way transmittance of the overlying layer(s) (appendix B in [Garnier et al., 2021a](#)). For single-layer *upper levels*, Integrated_Backscatter_Upper_Level is simply IAB reported by CALIOP. This parameter is set to a fill value when no IIR retrievals are attempted.

Layer_Top_Height_Upper_Level

Units: km

Format: Float_32

Valid Range: -0.5, 30.1

Fill Value: -9999.0

Description: Duplicate of the Lidar_Top_Altitude reported in the CALIOP Level 2 Cloud or Aerosol layer product for the uppermost layer in the *upper level*. Because the algorithm only accounts for features detected with 5 or 20 km horizontal averaging, the uppermost layer reported here can be lower than in the CALIOP product. This parameter is set to a fill value when no IIR retrievals are attempted.

Centroid_IAB_0532_Upper_Level

Units: km

Format: Float_32

Valid Range: -0.5, 30.1

Fill Value: -9999.0

Description: Centroid altitude of the CALIOP 532 nm attenuated backscatter profile for the *upper level*. For single-layer *upper levels*, this parameter is a duplicate of the centroid altitude provided in the Attenuated_Backscatter_Statistics_532 parameter reported in the CALIOP Level 2 Cloud and/or Aerosol layer products. For multi-layer *upper levels*, the centroid altitude is estimated as the weighted average of the centroid altitudes of the layers included in the *upper level*, by using as a weight for each layer the product of the 532-nm integrated attenuated backscatter and of the overlying 532-nm two-way transmittance (see appendix B in [Garnier et al., 2021a](#)). This parameter is set to a fill value when no IIR retrievals are attempted.

Layer_Bottom_Height_Upper_Level

Units: km

Format: Float_32

Valid Range: -0.5, 30.1

Fill Value: -9999.0

Description: Duplicate of the Layer_Base_Altitude reported in the CALIOP Level 2 Cloud or Aerosol layer product for the lowermost layer in the *upper level*. This parameter is set to a fill value when no IIR retrievals are attempted.

Layer_Top_Temperature_Upper_Level

Units: K

Format: Float_32

Valid Range: 160.0, 340.0

Fill Value: -9999.0

Description: Temperature at Layer_Top_Height_Upper_Level duplicated from the CALIOP Level 2 Cloud or Aerosol layer product. This parameter is set to a fill value when no IIR retrievals are attempted.

Temperature_Centroid_IAB_0532_Upper_Level

Units: K

Format: Float_32

Valid Range: 160.0, 340.0

Fill Value: -9999.0

Description: Centroid temperature of the *upper level* derived from Centroid_IAB_0532_Upper_Level and MERRA 2 profiles. This parameter is set to a fill value when no IIR retrievals are attempted.

Layer_Bottom_Temperature_Upper_Level

Units: K

Format: Float_32

Valid Range: 160.0, 340.0

Fill Value: -9999.0

Description: Temperature at Layer_Bottom_Height_Upper_Level duplicated from the CALIOP Level 2 Cloud or Aerosol layer product. This parameter is set to a fill value when no IIR retrievals are attempted.

Layer_Top_Pressure_Upper_Level

Units: hPa

Format: Float_32

Valid Range: 1.0, 1086.0

Fill Value: -9999.0

Description: Pressure at Layer_Top_Height_Upper_Level duplicated from the CALIOP Level 2 Cloud or Aerosol layer product. This parameter is set to a fill value when no IIR retrievals are attempted.

Pressure_Centroid_IAB_0532_Upper_Level

Units: hPa

Format: Float_32

Valid Range: 1.0, 1086.0

Fill Value: -9999.0

Description: Centroid pressure of the *upper level* derived from Centroid_IAB_0532_Upper_Level and MERRA 2 profiles. This parameter is set to a fill value when no IIR retrievals are attempted.

Layer_Bottom_Pressure_Upper_Level

Units: hPa

Format: Float_32

Valid Range: 1.0, 1086.0

Fill Value: -9999.0

Description: Pressure at Layer_Bottom_Height_Upper_Level duplicated from the CALIOP Level 2 Cloud or Aerosol layer product. This parameter is set to a fill value when no IIR retrievals are attempted.

Ice_Water_Flag_Upper_Level

Units: NoUnits

Format: Int_8

Valid Range: 1, 9

Fill Value: -99

Description: Ice/Water phase of the *upper level* built from the Ice/Water Phase of each layer of the *upper level* reported by the Feature Classification Flag in the CALIOP Level 2 Cloud layer product.

Table 5: Interpretation of Ice Water Flag Upper Level

Value	Description	Interpretation
1	CALIOP Ice/Water phase=1, all layers	randomly oriented ice crystals (ROI)
2	CALIOP Ice/Water phase=2, all layers	liquid water
3	CALIOP Ice/Water phase=3, all layers	horizontally oriented ice crystals (HOI)
4	CALIOP Ice/Water phase=1 and 3	ice crystals only, both ROI and HOI
6	CALIOP Ice/Water phase=(1 or 3) and 2	(ROI and/or HOI) ice and liquid water
9	at least one layer has CALIOP Ice/Water phase=0	at least one layer has unknown/not determined phase
-99	fill value	no cloud layer in <i>upper level</i> or retrievals not attempted

Ice_Water_Flag_QA_Upper_Level

Units: NoUnits

Format: Float_32

Valid Range: 0.0, 100.1

Fill Value: -9999.0

Description: Parameter built from the Feature Type QA and Ice/Water Phase QA reported by the Feature Classification Flag in the CALIOP Level 2 Cloud layer product for each layer of the *upper level*. The QA flags are converted into scores, chosen between 0 and 100. The Feature Type and Ice/Water Phase scores assigned to the *upper level* are the mean scores. Finally, the mean scores are combined into Ice_Water_Flag_QA_Upper_Level as:

$$\text{Feature_Type_score} + 0.001 \times \text{Ice/Water_Phase_score}$$

This parameter is a set to a fill value if the *upper level* does not contain cloud layers or if no retrievals are attempted, and to -99.00 if Type of Scene is -99.

Table 6: Interpretation of the Feature Type and Ice/Water Phase scores assigned to each level of the upper level to build Ice Water Flag QA Upper Level

Feature_Type_score	CALIOP Feature Type QA	Ice/Water_Phase_score	CALIOP Ice/Water Phase QA
100	high	100	high
50	medium	50	medium
25	low	25	low

Feature_Type_score	CALIOP Feature Type QA	Ice/Water_Phase_score	CALIOP Ice/Water Phase QA
0	none	0	none

Example: Ice_Water_Flag_QA_Upper_Level = 75.1 means: a) Feature_Type_score = 75 (medium to high confidence in the cloud/aerosol classification for the cloud layers included in the *upper level*) and b) Ice/Water_Phase_score = 100 (high confidence in the Ice/Water phase classification for all the cloud layers included in the *upper level*).

Ice_Water_Path_CALIOP_Upper_Level

Units: g/(m²)

Format: Float_32

Valid Range: 0.0, 500.0

Fill Value: -9999.0

Description: Summation of the layers ice water paths reported in the CALIOP Level 2 Cloud layer product for the ice layers included in the *upper level*. This parameter is set to a fill value when no effective emissivity retrievals are attempted.

Optical_Depth_0532_Lower_Level

Units: NoUnits

Format: Float_32

Valid Range: 0.0, 5.0

Fill Value: -9999.0

Description: Duplicate of the Feature_Optical_Depth_532 parameter reported in the CALIOP Level 2 Cloud or Aerosol layer product for the *lower level*, if any, according to Type_of_Scene. Otherwise, this parameter is set to a fill value.

Depolarization_Lower_Level

Units: NoUnits

Format: Float_32

Valid Range: 0.0, 1.0

Fill Value: -9999.0

Description: Duplicate of the Integrated_Part particulate_Depolarization_Ratio parameter reported in the CALIOP lidar Level 2 Cloud or Aerosol layer product for the *lower level*, if any, according to Type_of_Scene. Otherwise, this parameter is set to a fill value.

Integrated_Backscatter_Lower_Level

Units: 1/sr

Format: Float_32

Valid Range: 0.0, 1.0

Fill Value: -9999.0

Description: Duplicate of the Integrated_Attenuated_Backscatter_532 parameter reported in the CALIOP Level 2 Cloud or Aerosol layers product for the *lower level*, if any, according to Type_of_Scene. Otherwise, this parameter is set to a fill value.

Layer_Top_Height_Lower_Level

Units: km

Format: Float_32

Valid Range: -0.5, 30.1

Fill Value: -9999.0

Description: Duplicate of the Layer_Top_Altitude parameter reported in the CALIOP Level 2 Cloud or Aerosol layers product for the *lower level*, if any, according to Type_of_Scene. Otherwise, this parameter is set to a fill value.

Centroid_IAB_0532_Lower_Level

Units: km

Format: Float_32

Valid Range: -0.5, 30.1

Fill Value: -9999.0

Description: Duplicate of the centroid altitude provided in the Attenuated_Backscatter_Statistics_532 parameter reported in the CALIOP Level 2 Cloud or Aerosol layer product for the *lower level*, if any, according to Type_of_Scene. Otherwise, this parameter is set to a fill value.

Layer_Bottom_Height_Lower_Level

Units: km

Format: Float_32

Valid Range: -0.5, 30.1

Fill Value: -9999.0

Description: Duplicate of the Layer_Base_Altitude parameter reported in the CALIOP Level 2 Cloud or Aerosol layers product for the *lower level*, if any, according to Type_of_Scene. Otherwise, this parameter is set to a fill value.

Layer_Top_Temperature_Lower_Level

Units: K

Format: Float_32

Valid Range: 160.0, 340.0

Fill Value: -9999.0

Description: Temperature at Layer_Top_Height_Lower_Level duplicated from the CALIOP Level 2 Cloud or Aerosol layer product for the *lower level*, if any, according to Type_of_Scene. Otherwise, this parameter is set to a fill value.

Temperature_Centroid_IAB_0532_Lower_Level

Units: K

Format: Float_32

Valid Range: 160.0, 340.0

Fill Value: -9999.0

Description: Centroid temperature derived from Centroid_IAB_0532_Lower_Level and MERRA 2 profiles for the *lower level*, if any, according to Type_of_Scene. Otherwise, this parameter is set to a fill value.

Layer_Bottom_Temperature_Lower_Level

Units: K

Format: Float_32

Valid Range: 160.0, 340.0

Fill Value: -9999.0

Description: Temperature at Layer_Bottom_Height_Lower_Level duplicated from the CALIOP Level 2 Cloud or Aerosol layer product for the *lower level*, if any, according to Type_of_Scene. Otherwise, this parameter is set to a fill value.

Layer_Top_Pressure_Lower_Level

Units: hPa

Format: Float_32

Valid Range: 1.0, 1086.0

Fill Value: -9999.0

Description: Duplicate of the Layer_Top_Pressure parameter reported in the CALIOP Level 2 Cloud or Aerosol layer product for the *lower level*, if any, according to Type_of_Scene. Otherwise, this parameter is set to a fill value.

Pressure_Centroid_IAB_0532_Lower_Level

Units: hPa

Format: Float_32

Valid Range: 1.0, 1086.0

Fill Value: -9999.0

Description: Centroid pressure derived from Centroid_IAB_0532_Lower_Level and MERRA 2 profiles for the *lower level*, if any, according to Type_of_Scene. Otherwise, this parameter is set to a fill value.

Layer_Bottom_Pressure_Lower_Level

Units: hPa

Format: Float_32

Valid Range: 1.0, 1086.0

Fill Value: -9999.0

Description: Duplicate of the Layer_Base_Pressure parameter reported in the CALIOP Level 2 Cloud or Aerosol layer product for the *lower level*, if any, according to Type_of_Scene. Otherwise, this parameter is set to a fill value.

Ice_Water_Flag_Lower_Level

Units: NoUnits

Format: Int_8

Valid Range: -9, 9

Fill Value: -99

Description: Ice/Water phase of the *lower level* built from the Ice/Water Phase reported by the Feature Classification Flag in the CALIOP Level 2 Cloud layer product of the *lower level*, if any. In addition, this flag is assigned specific values if the *lower level* is an aerosol, and if the reference is the surface or no retrievals are attempted (i.e. no *lower level*).

Table 7: Interpretation of Ice Water Flag Lower Level

Value	CALIOP Ice/Water Phase	Interpretation
1	1	randomly oriented ice crystals (ROI)
2	2	liquid water
3	3	horizontally oriented ice crystals (HOI)
9	0	unknown/not determined

Value	CALIOP Ice/Water Phase	Interpretation
5	N/A	lower level is an aerosol layer
-9	N/A	background reference is the surface or retrievals not attempted
-99	N/A	type of Scene not defined (99 or -99)

Ice_Water_Flag_QA_Lower_Level

Units: NoUnits

Format: Float_32

Valid Range: 0.0, 100.1

Fill Value: -9999.0

Description: Parameter built from the Feature Type QA and Ice/Water Phase QA reported by the Feature Classification Flag in the CALIOP Level 2 Cloud layer product for the *lower level*. The QA flags are converted into scores, chosen between 0 and 100. If the *lower level* is an aerosol, then Ice/Water Phase is set to 0. The Feature Type and Ice/Water Phase scores are then combined into Ice_Water_Flag_QA_Lower_Level as:

$$\text{Feature_Type_score} + 0.001 \times \text{Ice/Water_Phase_score}.$$

This parameter is set to a fill value if there is no *lower level* and to -99.00 if Type of Scene is -99.

Table 8: Interpretation of the Feature Type and Ice/Water Phase scores assigned to the lower level to build Ice Water Flag QA Lower Level

Feature_Type_score	CALIOP Feature Type QA	Ice/Water_Phase_score	CALIOP Ice/Water Phase QA
100	high	100	high
50	medium	50	medium
25	low	25	low
0	none	0	None or aerosol

Surface_Emissivity_08_65

Surface_Emissivity_12_05

Surface_Emissivity_10_60

Units: NoUnits

Format: Float_32

Valid Range: 0.0, 1.0

Fill Value: -9999.0

Description: Surface emissivity for IIR channels 8.65, 12.05 and 10.6 determined according to the TGeotype category. For snow-free land and permanent-snow (IGBP Surface Type = 15) pixels, the 8.65 and 10.6 surface emissivities are determined using monthly nighttime and daytime maps (resolution: latitude x longitude = 1° x 2°) established from the analysis of IIR observations in clear sky conditions.

Table 9: Surface Emissivity determined by TGeotype category

Category	Surface Emissivity		
	08.65 μm	10.60 μm	12.05 μm
Water	0.971	0.984	0.982
Water/sea ice transition	0.981	0.990	0.982
Sea Ice	0.981	0.990	0.982
Snow (not permanent)	0.966	0.977	0.975
Snow-free land or permanent snow	Monthly Maps	Monthly Maps	0.975

IGBP_Surface_Type

Units: NoUnits

Format: Int_8

Valid Range: 1, 18

Fill Value: -99

Description: Duplicate of the IGBP_Surface_Type parameter reported in the CALIOP Level 2 layer products. Reports the IGBP (International Geosphere/Biosphere Program) surface type provided by the CERES/SARB surface map. This parameter is set to a fill value if Type of Scene is -99.

Table 10: Interpretation of the IGBP Surface Type values

Value	Surface Type	Value	Surface Type
1	Evergreen-Needleleaf-Forest	10	Grassland
2	Evergreen-Broadleaf-Forest	11	Wetland
3	Deciduous-Needleleaf-Forest	12	Cropland
4	Deciduous-Broadleaf-Forest	13	Urban
5	Mixed-Forest	14	Crop-Mosaic
6	Closed-Shrubland	15	Permanent-Snow
7	Open-Shrubland (Desert)	16	Barren/Desert
8	Woody-Savanna	17	Water
9	Savanna	18	Tundra

Snow_Ice_Surface_Type

Units: NoUnits

Format: Int_8

Valid Range: 0, 255

Fill Value: 99

Description: Duplicate of the Snow_Ice_Surface_Type parameter reported in the CALIOP Level 2 layer products. Reports the AFWA (Air Force Weather Agency) Snow and Ice map. Values between 0 and 100 represent the percentage of ice within a pixel having a nominal resolution of 25 km². Pixels with permanent ice are assigned a value of 101. A value of 103 indicates pixels containing snow. 255 indicates mixed type/uncertain type pixels at coastlines. A value of 99 is a fill value only when Type of Scene is -99.

Surface_532_Integrated_Depolarization_Ratio

Units: NoUnits

Format: Float_32

Valid Range: 0.0,1.0

Fill Value: -9999.0

Description: Duplicate of the Surface_532_Integrated_Depolarization_Ratio parameter reported in the CALIOP Level 2 layer products.

TGeotype

Units: NoUnits

Format: Int_16

Valid Range: 100,1800

Fill Value: -9999.0

Description: Parameter derived from IGBP_Surface_Type (IGBP), as well as Surface_532_Integrated_Depolarization_Ratio, if available, and otherwise Snow_Ice_Surface_Type, to identify pixels covered with sea ice or not permanent snow. The classification at coastlines (Snow_Ice_Surface_Type = 255) is evaluated only when the surface depolarization ratio is available. Otherwise, TGeotype at coastlines is IGBP x 100.

Table 11: Derivation of the TGeotype parameter

Category	TGeotype	Interpretation
Water	1700	IGBP water (17) Surface depolarization ratio < 0.15 or No surface depolarization and snow ice surface type = 0
	1705	IGBP water (17) No surface depolarization and 0 < snow ice surface type < 50
	1750	Coastline land (IGBP ≠ 17) pixel changed to water because surface depolarization ratio < 0.15
Water/sea ice transition	1710	IGBP water (17) 0.15 ≤ surface depolarization ratio ≤ 0.6
Sea ice	1510	IGBP water (17) Surface depolarization > 0.6 or No surface depolarization and snow ice surface type ≥ 50
Snow (not permanent)	1560	Land not permanent snow (IGBP ≠ 17 and ≠ 15) Surface depolarization > 0.6 or No surface depolarization and snow ice surface type ≥ 50
Snow-free land	IGBP x 100	Land not permanent snow (IGBP ≠ 17 and ≠ 15) Surface depolarization < 0.6 or No surface depolarization and snow ice surface type < 50
	1730	Coastline water (IGBP = 17) pixel changed to snow-free land because 0.15 ≤ surface depolarization ratio ≤ 0.6
Permanent snow	1500	IGBP = 15

Initial_Surface_Temperature

Units: K

Format: Float_32

Valid Range: 160.0, 340.0

Fill Value: -9999.0

Description: MERRA-2 skin temperature.

Surface_Temperature

Units: K

Format: Float_32

Valid Range: 160.0, 340.0

Fill Value: -9999.0

Description: Skin temperature used for the emissivity retrievals. For pixels located over snow-free land or permanent snow, the initial MERRA 2 skin temperature is corrected using monthly nighttime and daytime correction maps (resolution: latitude x longitude = 1° x 2°) established from the analysis of IIR observations in clear sky conditions.

IIR_Data_Quality_Flag

Units: NoUnits

Format: Int_8

Valid Range: 0, 15

Fill Value: -99

Description: Indicator of the IIR calibrated radiance quality extracted from the Pixel_Quality_Index of the IIR Level 1B product. If not zero, corresponding to nominal quality:

- either one channel has poor quality or is missing, or
- the radiances in the 3 channels are not all part of the same image measurement sequences which, for scenes with high broken clouds, could lead to some errors at the edge of the images for geometrical reasons.

Table 12: Interpretation of IIR Data Quality Flag

Bit	Bit Value	Interpretation
1	0	IIR calibrated radiances in the 3 channels are of nominal quality
	1	At least one of the channels has poor quality or is missing
2	0	Channels 08.65 and 10.60 derived from the same sequence of acquisition
	1	Channels 08.65 and 10.60 not derived from the same sequence of acquisition
3	0	Channels 08.65 and 12.05 derived from the same sequence of acquisition
	1	Channels 08.65 and 12.05 not derived from the same sequence of acquisition
4	0	Channels 10.60 and 12.05 derived from the same sequence of acquisition
	1	Channels 10.60 and 12.05 not derived from the same sequence of acquisition
5-8	N/A	N/A

Equalization_Flag

Units: NoUnits

Format: Int_8

Valid Range: 0, 7

Fill Value: -99

Description: Indicator of whether an equalization correction has been applied, extracted from the Pixel_Quality_Index of the IIR Level 1B product.

Table 13: Interpretation of Equalization Flag

Bit	Bit Value	Interpretation Equalization Correction
1	0	Channel 12.05: no
	1	Channel 12.05: yes
2	0	Channel 10.60: no
	1	Channel 10.60: yes
3	0	Channel 08.65: no
	1	Channel 08.65: yes
4-8	N/A	N/A

LIDAR_Data_Quality_Flag

Units: NoUnits

Format: Int_8

Valid Range: 0, 3

Fill Value: -99

Description: Feature Type QA derived from the Feature_Classification_Flag parameter reported in the CALIOP lidar Level 2 layer products for the uppermost layer in the *upper level*.

Table 14: Interpretation of LIDAR Data Quality Flag

Value	Interpretation
0	none
1	low
2	medium
3	high

Surrounding_Obs_Quality_Flag

Units: NoUnits

Format: Int_16

Valid Range: 0, 412

Fill Value: -9999

Description: Composite of three different pieces of information: (1) The units digit indicates if the studied pixel is isolated or part of a structure with consecutive IIR pixels of same Type_of_Scene. It is not computed for scenes containing only aerosols, for type of scene 20, or when no IIR retrievals are attempted. (2) The tens digit is a mineral aerosols index based on IIR inter-channels brightness temperature differences (BTD). Mineral aerosols layers are identified (tens digit = 1) when the 08_65 minus 12_05 BTD is < -2 K and the 10_60 minus 12_05 BTD is < -0.5 K, (3) The hundreds digit is an index describing the difference between observed and computed brightness temperatures for specific types of scenes: scenes identified as clear sky

(10) or containing low aerosols (52, 53) and scenes containing opaque clouds (20, 40). This index is designed to identify cloud-free and opaque cloud pixels where measured and computed brightness temperatures are exhibiting large differences, and which may require further analysis.

Table 15: Interpretation Surrounding Obs Quality Flag

Digit	Digit Value	Digit Interpretation
Units	0	3 or more consecutive pixels with the same Type_of_Scene
	1	2 consecutive pixels with the same Type_of_Scene
	2	Not computed
Tens IIR aerosols index	0	No mineral aerosols detected
	1	Mineral aerosols detected
Hundreds Obs-Computed BTs	0	Not computed or satisfactory for computed cases: Mean (Observed - Computed) Brightness Temperatures between -2K and +2K
	1	Low Mean (Observed - Computed) Brightness Temperatures between -5K and -2K
	2	High Mean (Observed - Computed) Brightness Temperatures between +2K and +5K
	3	Very low Mean (Observed - Computed) Brightness Temperatures < -5K
	4	Very high Mean (Observed - Computed) Brightness Temperatures > 5K

High_Cloud_vs_Background_Flag

Units: NoUnits

Format: Float_32

Valid Range: -93.0, 412.0

Fill Value: -9999.0

Description: Provides the main characteristics of the background radiances used to retrieve the effective emissivity of the current pixel. If the background radiance is derived from reference measurements in the vicinity of the pixel, the unit digit gives an indication of the mean distance from the current pixel. If it is derived from the FASRAD model, the unit digit is set to zero. Depending on Type_of_Scene, the reference can be clear sky (10) or possibly low transparent non-depolarizing aerosols (52), a low opaque cloud (20), a high opaque cloud (40), or a low opaque aerosols layer (56). This information is provided in the hundreds digit. When the reference is a cloud or aerosol layer selected among nearby observations (i.e. not computed), the tens digit indicates the range of values of its effective emissivity. Otherwise, it is set to 0 (computed reference) or -9 (clear sky reference).

Table 16: Interpretation of High Cloud vs. Background Flag

Digit	Digit Value	Digit Interpretation
Units	0	Background reference computed
	1	Background reference measured at a distance <= 10 km
	2	Background reference measured, 10 km < distance <= 50 km

Digit	Digit Value	Digit Interpretation
	3	Background reference measured, 50 km < distance <= 100 km
Tens	0	Background reference computed
	1	Measured background reference effective emissivity between -0.1 and 1.1
	2	Measured background reference effective emissivity < -0.1
	3	Measured background reference effective emissivity > 1.1
	-9	Measured background reference is clear sky
Hundreds	0	Background reference: clear sky (10)
	1	Background reference: low opaque cloud (20)
	2	Background reference: high opaque cloud (40)
	3	Background reference: low semi-transparent non-depolarizing aerosols (52)
	4	Background reference: low opaque aerosol layer (56)

Computed_vs_Observed_Flag

Units: NoUnits

Format: Float_32

Valid Range: -10.0, 10.0

Fill Value: -9999.0

Description: Assesses the impact of computed versus measured background reference radiances in the retrieved effective emissivities. If the background reference is derived from a series of neighboring pixels (cf High_Cloud_vs_Background_Flag), this parameter gives the mean relative difference between those measurements and the computed radiances (not used to retrieve the effective emissivities). Otherwise, the parameter is set to a fill value. The three elements are for the IIR channels 08.65, 10.60 and 12.05 respectively.

Regional_Background_Std_Dev_Flag

Units: NoUnits

Format: Float_32

Valid Range: 0.0, 1.0

Fill Value: -9999.0

Description: Assesses the standard deviation associated to Computed_vs_Observed_Background_Flag: 0 = standard deviation < 0.15; 1 = standard deviation > 0.15.

Microphysics

Units: NoUnits

Format: Float_32

Valid Range: 0.0, 2002009.0

Fill Value: -9999.0

Description: Provides the whole set of $D_{e12/10}$ and $D_{e12/08}$ diameters inferred from the $\beta_{eff12/10}$ and $\beta_{eff12/08}$ microphysical indices as derived from the V3 LUTs (records 1 to 3) and the identical V4 and V5 LUTs (records 4 to 6). In addition, records 7 to 10 are $D_{e12/10}$ derived from four initial relationships used in the V4 algorithm established using in-situ aircraft data during the SPARTICUS and TC4 campaigns (Table 1 in Mitchell et al. (2018)). Because of uncertainties in the first bin $N(D)_1$ of the size distributions, two LUTs were established for each campaign, with $N(D)_1$ unmodified or set to zero.

Table 17: Description of the Microphysics derivation and interpretation

Digit	Digit Interpretation
Units	Records 1 to 3: particle shape_index used in V3 (7: Aggregate, 8: Plate, 9: Solid column, see Yang et al., 2005). Records 4 to 6: particle shape_index. Records 7 to 10: set to 0.
Thousands-Hundreds-Tens	Effective diameter $D_{e12/08}$ in microns Records 1 to 3: V3. Records 4 to 6: set to zero if $\beta_{eff12/08}$ is not valid and $\beta_{eff12/10}$ is valid. Records 7 to 10: set to 0.
Millions-Hundred thousands-Ten thousands	Effective diameter $D_{e12/10}$ in microns Records 1 to 3: V3. Records 4 to 6: set to zero if $\beta_{eff12/10}$ is not valid and $\beta_{eff12/08}$ is valid. Records 7 to 10: V4 SPARTICUS $N(D)_1$ unmodified, TC4 $N(D)_1$ unmodified, SPARTICUS $N(D)_1 = 0$, TC4 $N(D)_1 = 0$.

Dust_Stratospheric_Aerosol_Flag

Units: NoUnits

Format: Int_8

Valid Range: 0,8

Fill Value: -99

Description: Records the number of aerosol layers in the atmospheric column classified by CALIOP as: record #1: tropospheric dust, record #2: tropospheric polluted dust, record #3: tropospheric dusty marine, record #4: polar stratospheric aerosol, record #5: stratospheric volcanic ash, record #6: stratospheric sulfate, and record #7: stratospheric elevated smoke.

Dust_Stratospheric_Aerosol_Flag_QA

Units: NoUnits

Format: Float_32

Valid Range: 0.0,100.1

Fill Value: -9999.0

Description: Records the QA scores assigned to the seven aerosol subtypes reported in Dust_Stratospheric_Aerosol_Flag. For each aerosol subtype, the QA score is computed from Feature Type QA and Aerosol Type QA reported in the parameter Feature_Classification_Flags in the CALIOP Level 2 Aerosol layer product. Feature Type QA and Aerosol Type QA of each layer are converted into scores, chosen between 0 and 100. The Feature Type and Aerosol Type scores assigned to the atmospheric column are the mean scores. Finally, the mean scores are combined into Dust_Stratospheric_Aerosol_Flag_QA as $Feature_Type_score + 0.001 \times Aerosol_Type_score$.

Table 18: Interpretation of the Feature Type and Aerosol Type scores assigned to the selected aerosol layers in the column to build Dust Stratospheric Aerosol Flag QA

Feature_Type_Score	CALIOP Feature Type QA	Aerosol_Type_Score	CALIOP Aerosol Type QA
100	high	100	confident
50	medium		

Feature_Type_Score	CALIOP Feature Type QA	Aerosol_Type_Score	CALIOP Aerosol Type QA
25	low		
0	none	0	not confident

Reflectance

Units: NoUnits

Format: Float_32

Valid Range: 0.0, 2.0

Fill Value: -9999.0

Description: Wide Field of view Camera (WFC) reflectance duplicated from the IIR WFC Level 1B product.

Integrated_Water_Vapor_Path

Units: g/(cm²)

Format: Float_32

Valid Range: 0.0, 10.0

Fill Value: -9999.0

Description: Column-integrated atmospheric water vapor derived from the MERRA 2 product.

Radiative_Temperature_Upper_Level

Units: K

Format: Float_32

Valid Range: 160.0, 340.0

Fill Value: -9999.0

Description: Temperature associated with the top of atmosphere blackbody brightness temperature at 12.05 μm used to retrieve the effective emissivity of the *upper level* at 12.05 μm (see Blackbody_Brightness_Temperature). When the *upper level* is composed of semi-transparent ice clouds, this temperature corresponds to the radiance obtained from equation 5 in [Garnier et al., 2021a](#), where the in-cloud temperature and extinction profiles are from the CALIOP cloud profile product. When the *upper level* is an opaque ice cloud, this temperature is derived from the V4 parameterized functions described in Section 3.4.2 of [Garnier et al., 2021a](#). In all the other cases, this temperature is Temperature_Centroid_IAB_0532_Upper_Level.

Radiative_Height_Upper_Level

Units: km

Format: Float_32

Valid Range: -0.5, 30.1

Fill Value: -9999.0

Description: Altitude corresponding to Radiative_Temperature_Upper_Level as derived using the MERRA 2 profiles.

Radiative_Pressure_Upper_Level

Units: hPa

Format: Float_32

Valid Range: 1.0, 1086.0

Fill Value: -9999.0

Description: Pressure corresponding to Radiative_Temperature_Upper_Level as derived using the MERRA 2 profiles.

Cloud_Optical_Depth

Units: NoUnits

Format: Float_32

Valid Range: 0.0, 20.0

Fill Value: -9999.0

Description: Cloud visible optical depth reported when the *upper level* includes only ice clouds or only water clouds (see equation 11b and section 5.2 in [Garnier et al., 2021a](#)). Otherwise, this parameter is set to a fill value.

Cloud_Optical_Depth_Uncertainty

Units: NoUnits

Format: Float_32

Valid Range: 0.0, 20.0

Fill Value: -9999.0

Description: Estimated absolute uncertainty in the optical depth reported in Cloud_Optical_Depth.

Cirrus_IIR_Thickness

Units: km

Format: Float_32

Valid Range: 0.0,30.6

Fill Value: -9999.0

Description: IIR equivalent layer thickness derived using the temperature and extinction profiles reported in the CALIOP cloud profile product (see section 6.1 in [Garnier et al., 2021a](#)); reported when the *upper level* is semi-transparent to CALIOP and includes only ice clouds.

Cirrus_Number_Concentration

Units: 1/L

Format: Float_32

Valid Range: 0.0, 1000000.0

Fill Value: -9999.0

Description: Layer number concentration derived using relationships with the $\beta_{\text{eff}12/10}$ microphysical index that were established using in-situ aircraft data (see section 2.1, table 3, and table 5 in [Mitchell et al., 2025](#)); reported when the *upper level* is semi-transparent to CALIOP and includes only ice clouds. is semi-transparent to CALIOP and includes only ice clouds.

Cirrus_Number_Concentration_Uncertainty

Units: 1/L

Format: Float_32

Valid Range: 0.0, 1000000.0

Fill Value: -9999.0

Description: Estimated absolute uncertainty in the number concentration reported in Cirrus_Number_Concentration (see appendix B in [Mitchell et al., 2025](#)).

Cirrus_IIR_Extinction

Units: 1/km

Format: Float_32

Valid Range: 0.0, 60.0

Fill Value: -9999.0

Description: Layer visible extinction seen by IIR derived using relationships with the $\beta_{\text{eff}12/10}$ microphysical index that were established using in-situ aircraft data (see section 2.1, table 3, and table 5 in [Mitchell et al., 2025](#)); reported when the *upper level* is semi-transparent to CALIOP and includes only ice clouds.

Cirrus_IIR_Extinction_Uncertainty

Units: 1/km

Format: Float_32

Valid Range: 0.0, 60.0

Fill Value: -9999.0

Description: Estimated absolute uncertainty in the extinction reported in Cirrus_IIR_Extinction (see appendix B in [Mitchell et al., 2025](#)).

Cirrus_Optical_Depth

Units: NoUnits

Format: Float_32

Valid Range: 0.0, 20.0

Fill Value: -9999.0

Description: Visible optical depth derived using relationships with the $\beta_{\text{eff}12/10}$ microphysical index that were established using in-situ aircraft data (see section 2.1, table 3, and table 5 in [Mitchell et al., 2025](#)); reported when the *upper level* is semi-transparent to CALIOP and includes only ice clouds.

Cirrus_Optical_Depth_Uncertainty

Units: NoUnits

Format: Float_32

Valid Range: 0.0, 20.0

Fill Value: -9999.0

Description: Estimated absolute uncertainty in the optical depth reported in Cirrus_Optical_Depth (see appendix B in [Mitchell et al., 2025](#)).

Cirrus_Effective_Diameter

Units: μm

Format: Float_32

Valid Range: 0.0, 150.0

Fill Value: -9999.0

Description: Effective diameter derived using relationships with the $\beta_{\text{eff}12/10}$ microphysical index that were established using in-situ aircraft data (see section 2.1, table 3, and table 5 in [Mitchell et al., 2025](#)); reported when the *upper level* is semi-transparent to CALIOP and includes only ice clouds.

Cirrus_Effective_Diameter_Uncertainty

Units: μm

Format: Float_32

Valid Range: 0.0,150.0

Fill Value: -9999.0

Description: Estimated absolute uncertainty in the effective diameter reported in Cirrus_Effective_Diameter (see appendix B in [Mitchell et al., 2025](#)).

Cirrus_Ice_Water_Content

Units: mg/(m³)

Format: Float_32

Valid Range: 0.0,3000.0

Fill Value: -9999.0

Description: Layer ice water content derived using relationships with the $\beta_{\text{eff}12/10}$ microphysical index that were established using in-situ aircraft data (see section 2.1, table 3, and table 5 in [Mitchell et al., 2025](#)); reported when the *upper level* is semi-transparent to CALIOP and includes only ice clouds.

Cirrus_Ice_Water_Content_Uncertainty

Units: mg/(m³)

Format: Float_32

Valid Range: 0.0,3000.0

Fill Value: -9999.0

Description: Estimated absolute uncertainty in the ice water content reported in Cirrus_Ice_Water_Content (see Appendix B in [Mitchell et al., 2025](#)).

Cirrus_Ice_Water_Path

Units: g/(m²)

Format: Float_32

Valid Range: 0.0, 1000.0

Fill Value: -9999.0

Description: Ice water path derived using relationships with the $\beta_{\text{eff}12/10}$ microphysical index that were established using in-situ aircraft data (see section 2.1, table 3, and table 5 in [Mitchell et al., 2025](#)); reported when the *upper level* is semi-transparent to CALIOP and includes only ice clouds.

Cirrus_Ice_Water_Content_Uncertainty

Units: g/(m²)

Format: Float_32

Valid Range: 0.0, 1000.0

Fill Value: -9999.0

Description: Estimated absolute uncertainty in the ice water path reported in Cirrus_Ice_Water_Path (see appendix B in [Mitchell et al., 2025](#)).

Cirrus_Volume_Radius

Units: μm

Format: Float_32

Valid Range: 0.0, 100.0

Fill Value: -9999.0

Description: Volume radius derived using relationships with the $\beta_{\text{eff}12/10}$ microphysical index that were established using in-situ aircraft data (see section 2.1, table 3, and table 5 in [Mitchell et al., 2025](#)); reported when the *upper level* is semi-transparent to CALIOP and includes only ice clouds.

Cirrus_Volume_Radius_Uncertainty

Units: um

Format: Float_32

Valid Range: 0.0, 100.0

Fill Value: -9999.0

Description: Estimated absolute uncertainty in the volume radius reported in Cirrus_Volume_Radius (see appendix B in [Mitchell et al., 2025](#)).

Low_Energy_Mitigation_Column_QC_Flag

Units: NoUnits

Format: UInt_16

Valid Range: 0, 63

Fill Value: 9999

Description: In mid-2016, the CALIOP laser began intermittently emitting low energy laser pulses, and the occurrence frequency of these pulses slowly increased as the mission progressed. For the version 5.00 data release, CALIOP's low energy mitigation algorithm (LEM; [Tackett et al., 2025](#)) was enhanced for use in the level 2 data processing. The LEM algorithm identifies level 1 backscatter data resulting from low energy pulses and, when appropriate, excludes it from the level 2 analyses. The low energy mitigation column quality control (QC) flag is a bit-mapped 16-bit integer that summarizes the operation of the LEM algorithm within each 5 km vertical column in the CALIOP profile products.

Table 19: Interpretation of Low Energy Mitigation Column QC Flag

bit	interpretation
0	Column contains LEM affected data (data has been rejected or contains low energy shots that LEM accepts)
1	Column belongs to a 5 km resolution frame that has been rejected due to too many unusable profiles
2	Column belongs to a 5 km resolution frame that has been rejected due to too many rejected subregions in altitude region 3
3	Column belongs to a 5 km resolution frame that has been rejected due to too many rejected subregions in altitude region 4
4	Feature detection at 20 km resolution not performed in this column due to an insufficient fraction of usable 5 km resolution frames
5	Feature detection at 80 km resolution not performed in this column due to an insufficient fraction of usable 5 km resolution frames
6–15	unused

Metadata Parameter Descriptions

Product_ID

An 80-byte character string containing the product name. For the IIR Level 2 track products, the value of this string is "CAL_IIR_L2_Track".

Date_Time_at_Granule_Start

A 27-byte character string that specifies the granule start date and time. The format is yyyy-mm-ddThh:nn:ss.ffffffZ, where yyyy is the year, mm is the month, dd is the day, hh is the hour, nn is the minute, ss is the second, and fffffff is the fractional second. Date and time are separated by the character 'T'. The 'Z' indicates that time is given in UTC.

Date_Time_at_Granule_End

A 27-byte character string that specifies the granule end date and time. The format is yyyy-mm-ddThh:nn:ss.ffffffZ, where yyyy is the year, mm is the month, dd is the day, hh is the hour, nn is the minute, ss is the second, and fffffff is the fractional second. Date and time are separated by the character 'T'. The 'Z' indicates that time is given in UTC.

Date_Time_of_Production

A 27-byte character string that specifies the date and time at granule production. The format is yyyy-mm-ddThh:nn:ss.ffffffZ, where yyyy is the year, mm is the month, dd is the day, hh is the hour, nn is the minute, ss is the second, and fffffff is the fractional second. Date and time are separated by the character 'T'. The 'Z' indicates that time is given in UTC.

Initial_IIR_Scan_Center_Latitude

This field reports the first subsatellite latitude of the granule.

Initial_IIR_Scan_Center_Longitude

This field reports the first subsatellite longitude of the granule.

Ending_IIR_Scan_Center_Latitude

This field reports the last subsatellite latitude of the granule.

Ending_IIR_Scan_Center_Longitude

This field reports the last subsatellite longitude of the granule.

Orbit_Number_at_Granule_StartOrbit_Number_at_Granule_EndOrbit_Number_Change_Time

Orbit Number consists of three fields that define the number of revolutions by the CALIPSO spacecraft around the Earth. This number is incremented each time the spacecraft passes the equator on the ascending node. To maintain consistency between the CALIPSO and CloudSat orbit parameters, the Orbit Number is keyed to the CloudSat orbit 2121 at 23:00:47 on 2006/09/20. Because the CALIPSO data granules are organized according to the day and night conditions, based on fixed Sun-Earth-Satellite angles, day/night boundaries do not coincide with transition points for defining orbit number. As such, three parameters are needed to describe the orbit number for each granule as:

- **Orbit Number at Granule Start:** orbit number at the granule start time.
- **Orbit Number at Granule End:** orbit number at the granule stop time.
- **Orbit Number Change Time:** time at which the orbit number changes in the granule.

Path_Number_at_Granule_Start

Path_Number_at_Granule_Stop

Path_Number_Change_Time

Path Number consists of three fields that define an index ranging from 1-233 that references orbits to the Worldwide Reference System (WRS). This global grid system was developed to support scene identification for LandSat imagery. Since the A-Train is maintained to the WRS grid within +/- 10 km, the Path Number provides a convenient index to support data searches, instead of having to define complex latitude and longitude regions along the orbit track. The Path Number is incremented after the maximum latitude in the orbit is attained and changes by a value of 16 between successive orbits. Because the CALIPSO data granules are organized according

to the day and night conditions, based on fixed Sun-Earth-Satellite angles, day/night boundaries do not coincide with transition points for defining path number. As such, three parameters are needed to describe the path number for each granule as:

- **Path Number at Granule Start:** path number at the granule start time.
- **Path Number at Granule End:** path number at the granule stop time.
- **Path Number Change Time:** time at which the path number changes in the granule.

While CALIPSO was formation flying in the A-Train all path numbers in the metadata are exact. Beginning in September 2018, when CALIPSO lowered its orbit into the C-Train, path numbers are no longer exact, but they instead indicate the closest WRS reference orbit.

Number_of_IIR_Records_in_File

Number of IIR records in the file.

Number_of_Valid_08_65_Pixels

Number of pixels in the file with valid radiance in IIR channel 8.65.

Number_of_Valid_12_05_Pixels

Number of pixels in the file with valid radiance in IIR channel 12.05.

Number_of_Valid_10_60_Pixels

Number of pixels in the file with valid radiance in IIR channel 10.6.

Number_of_Invalid_08_65_Pixels

Number of pixels in the file with invalid radiance in IIR channel 8.65.

Number_of_Invalid_12_05_Pixels

Number of pixels in the file with invalid radiance in IIR channel 12.05.

Number_of_Invalid_10_60_Pixels

Number of pixels in the file with invalid radiance in IIR channel 10.6.

Number_of_Rejected_08_65_Pixels

Number of pixels in the file in IIR channel 8.65 rejected by the algorithm.

Number_of_Rejected_12_05_Pixels

Number of pixels in the file in IIR channel 12.05 rejected by the algorithm.

Number_of_Rejected_10_60_Pixels

Number of pixels in the file in IIR channel 10.6 rejected by the algorithm.

Number_of_Rejected_08_65_Pixels_Location

Number of pixels in the file in IIR channel 8.65 rejected by the algorithm due to co-location.

Number_of_Rejected_12_05_Pixels_Location

Number of pixels in the file in IIR channel 12.05 rejected by the algorithm due to co-location.

Number_of_Rejected_10_60_Pixels_Location

Number of pixels in the file in IIR channel 10.6 rejected by the algorithm due to co-location.

Number_of_Rejected_08_65_Pixels_Radiance

Number of pixels in the file in IIR channel 8.65 rejected by the algorithm due to radiance.

Number_of_Rejected_12_05_Pixels_Radiance

Number of pixels in the file in IIR channel 12.05 rejected by the algorithm due to radiance.

Number_of_Rejected_10_60_Pixels_Radiance

Number of pixels in the file in IIR channel 10.6 rejected by the algorithm due to radiance.

Mean_08_65_Radiance_All

Mean radiance (in $W/((m^2) \cdot sr \cdot \mu m)$) in the file in IIR channel 8.65 for the non-rejected pixels.

Mean_12_05_Radiance_All

Mean radiance (in $W/((m^2) \cdot sr \cdot \mu m)$) in the file in IIR channel 12.05 for the non-rejected pixels.

Mean_10_60_Radiance_All

Mean radiance (in $W/((m^2) \cdot sr \cdot \mu m)$) in the file in IIR channel 10.6 for the non-rejected pixels.

Mean_08_65_Radiance_Selected_Cases

Mean radiance (in $W/((m^2) \cdot sr \cdot \mu m)$) in the file in IIR channel 8.65 for the cases selected for emissivity retrievals.

Mean_12_05_Radiance_Selected_Cases

Mean radiance (in $W/((m^2) \cdot sr \cdot \mu m)$) in the file in IIR channel 12.05 for the cases selected for emissivity retrievals.

Mean_10_60_Radiance_Selected_Cases

Mean radiance (in $W/((m^2) \cdot sr \cdot \mu m)$) in the file in IIR channel 10.6 for the cases selected for emissivity retrievals.

Mean_08_65_Brightness_Temp_All

Mean brightness temperature (in Kelvin) in the file in IIR channel 8.65 for non-rejected pixels.

Mean_12_05_Brightness_Temp_All

Mean brightness temperature (in Kelvin) in the file in IIR channel 12.05 for non-rejected pixels.

Mean_10_60_Brightness_Temp_All

Mean brightness temperature (in Kelvin) in the file in IIR channel 10.6 for non-rejected pixels.

Mean_08_65_Brightness_Temp_Selected_Cases

Mean brightness temperature (in Kelvin) in the file in IIR channel 8.65 for the cases selected for emissivity retrievals.

Mean_12_05_Brightness_Temp_Selected_Cases

Mean brightness temperature (in Kelvin) in the file in IIR channel 12.05 for the cases selected for emissivity retrievals.

Mean_10_60_Brightness_Temp_Selected_Cases

Mean brightness temperature (in Kelvin) in the file in IIR channel 10.6 for the cases selected for emissivity retrievals.

Number_of_Valid_LIDAR_Pixels

Number of records in the lidar input product available at IIR pixel resolution.

Number_of_Invalid_LIDAR_Pixels

This field is set to 0.

Number_of_Rejected_LIDAR_Pixels

This field is set to 0.

Number_of_Selected_Cloud_Cases

Number of pixels in the file selected for emissivity retrievals with at least one cloud layer.

Percent_of_Selected_Cloud_Cases

Percentage of pixels in the file selected for emissivity retrievals with at least one cloud layer.

Number_of_Selected_Aerosol_Cases

Number of pixels in the file selected for emissivity retrievals with only aerosol layers.

Percent_of_Selected_Aerosol_Cases

Percentage of pixels in the file selected for emissivity retrievals with only aerosol layers.

Number_of_Identified_Pixels_Clear_Sky

Number of “clear sky” pixels in the file (i. e no clouds and no aerosols).

Percent_of_Identified_Pixels_Clear_Sky

Percentage of “clear sky” pixels in the file (i. e no clouds and no aerosols).

Mean_Altitude_High_Cloud

Mean centroid altitude (in km) for high clouds retrievals.

GEOS_Version

Specifies the version of the meteorological data used in the analyses. For the version 5.0 data release, this field is always “MERRA2”.

Data Release Information

Table 20: Dates, versions, and production strategy for all CALIPSO IIR level 2 data releases

IIR Level 2 Track and Swath, half orbit (Day and Night)			
Release Date	Version	Data Date Range	Production Strategy
October 2025	5.00	June 13, 2006 to June 30, 2023	Standard
October 2023	4.51	June 13, 2006 to June 30, 2023	Standard
October 2020	4.21	July 1, 2020 to January 19, 2022	Standard

April 2020	4.20	June 13, 2006 to June 30, 2020	Standard
October 2020	3.46	October 1, 2020 to June 30, 2023	Beta
September 2018	3.45	September 1, 2018 to September 30, 2020	Beta
December 2016	3.40	December 1, 2016 to August 31, 2018	Beta
August 2013	3.30	March 1, 2013 to November 30, 2016	Beta
December 2011	3.02	November 1, 2011 to February 28, 2013	Beta
May 2011	3.01	June 13, 2006 to October 31, 2011	Beta
October 2008	2.02	September 14, 2008 to January 17, 2011	Beta
October 2008	2.01	June 13, 2006 to September 13, 2008	Beta

Data Quality Information

Data Quality Statement for the release of the CALIPSO IIR Level 2 Product Version 5.00

The IIR level 2 Version 5.00 (V5) algorithm uses the new Version 3.00 IIR level 1B products while the previous IIR level 2 V4.51 algorithm (V4) used the previous Version 2. A new IIR level 1B version was generated to accommodate new code that generated two new public products, namely the IIR Level 1 Calibration and IIR Level 1 Calibration Correction data products. There was no change to the IIR Level 1B science algorithm and the reported brightness temperatures are identical in IIR level 2 V5 and V4 data products.

For this V5 data release, the suitable types of scenes for IIR retrievals are classified using the V5 CALIOP 5-km Cloud and Aerosol 5-km layer products. We recall that the retrievals are applied to the so-called *upper level* which includes either one single semi-transparent or opaque layer, or several semi-transparent layers. The V5 algorithm uses for the first time the temperature and extinction profiles reported in the V5 CALIOP cloud profile product to improve radiative temperature estimates and to produce a new series of retrievals when the *upper level* is composed of semi-transparent ice clouds (new parameter names starting with “Cirrus”).

The main algorithm changes implemented in V5 are in the track algorithm. They are listed below and are then described and assessed in more details:

- Changes related to the CALIOP Low Energy Mitigation algorithm implemented in the CALIOP V5 level 2 products,
- Adjustments related to the surface emissivity and surface temperature correction maps,
- Addition of the radiative temperature of the *upper level* with improved estimates in transparent ice clouds,
- Addition of radiative height and pressure associated with radiative temperature of the *upper level*,

- Addition of cloud optical depth and estimated uncertainty,
- Addition of a suite of new “cirrus” retrievals in transparent ice clouds and estimated uncertainties.

Changes related to the CALIOP Low Energy Mitigation algorithm

Over the last seven years of the mission, the CALIOP laser experienced an increasing frequency of shots with low to zero energy, which were initially prevalently located over the South Atlantic Anomaly and were then observed more globally at the end of the mission. A low energy mitigation (LEM) algorithm ([Tackett et al., 2025](#)) is implemented in the CALIOP Level 2 V5 products, which identifies level 1 backscatter data resulting from low energy pulses and, when appropriate, excludes it from the level 2 analyses. The CALIOP Low_Energy_Mitigation_Column_QC_Flag parameter, which summarizes the operation of the LEM algorithm within each 5 km vertical column in the CALIOP profile products, is duplicated in the IIR track product.

As in the previous versions, the scenes with lidar data that do not match the prescribed classification are reported as Type_of_Scene = 99. For this version 5.00 data release, the IIR pixels in 5-km columns that are rejected by the LEM algorithm fall into that category. The 5-km columns including low energy shots and accepted by the LEM algorithm are considered of nominal quality. The Low_Energy_Mitigation_Column_QC_Flag parameter can be used for further quality filtering if deemed necessary.

In V4, the “Was_Cleared_Flag_1km” parameter reported the number of clouds seen by the 1-km IIR pixel that were detected by CALIOP at single shot resolution and that were cleared from the CALIOP 5-km layer products (noted *number_cleared_shots*). In V5, Was_Cleared_Flag_1km contains also the number of single shot profiles seen by the 1-km IIR pixel that were rejected by the LEM algorithm (noted *number_rejected_profiles*). This flag is now built as:

$$\text{Was_Cleared_Flag_1km} = 10 \times \text{number_rejected_profiles} + \text{number_cleared_shots}$$

Both *number_cleared_shots* and *number_rejected_profiles* are between 0 and 3 and their sum is necessarily smaller than or equal to 3. When no single shot profiles were rejected by LEM, the interpretation of the flag is unchanged compared to V4. As in V4, the cloud-free (clear sky or aerosol only) scenes must have Was_Cleared_Flag_1km = 0. Indeed, scenes having Was_Cleared_Flag_1km = 10, 20, or 30 have 1 to 3 single-shot profiles rejected by the LEM algorithm and the presence of small-scale cloud(s) is unknown. Similarly, it is recommended, as in V4, to ensure that Was_Cleared_Flag_1km = 0 for detailed analyses of retrievals in optically thin clouds.

Surface emissivity and surface temperature corrections maps

The monthly maps (resolution: latitude x longitude = 1° x 2°) of surface emissivity at 8.65 and 10.6 μm and of surface temperature correction introduced in V4 were augmented near the coasts to account for orbital drifts after CALIPSO joined the C-Train in October 2018. The new coastal values were derived using neighboring pixels over land. In addition, a small inaccuracy of the latitude and longitude values used to read the maps was fixed in V5. This caused a pixel located at the border of two grid cells to be possibly assigned a wrong set of surface values. Overall, after these changes, less than 0.2 % of the pixels are assigned different surface parameters in V5 and in V4.

Radiative temperature of the upper level with improved estimates in transparent ice clouds

The radiative temperature of the upper level is the temperature used to compute the top of atmosphere blackbody brightness temperature at 12.05 μm, which is required to retrieve the effective emissivity of the upper level at 12.05 μm. Even though it could be retrieved by the user from Temperature_Centroid_IAB_0532_Upper_Level augmented by the difference between the 6th and 3rd records of the Blackbody_Brightness_Temperature parameter, it is now reported for clarity.

In V4, this temperature was derived from the V4 parameterized functions described in Section 3.4.2 of [Garnier et al. \(2021a\)](#) when the upper level was composed of ice clouds. Otherwise, this temperature was Temperature_Centroid_IAB_0532_Upper_Level.

For this V5 release, when the upper level is composed of semi-transparent ice clouds, this temperature corresponds to the radiance obtained from equation 5 in [Garnier et al. \(2021a\)](#), where the in-cloud temperature and extinction profiles are from the CALIOP V5 cloud profile product. This equation was used to determine the V4 parameterized functions, and it is instead now applied for each sample. Figure 1 compares the V4.51 and the V5 radiative temperatures for the month of April 2010 and statistics are given in Table 21. Both retrievals are in good agreement overall, with a larger dispersion for multi-layer upper levels for which both the initial estimate of the centroid temperature and the V4 parameterized functions could yield larger errors than in single-layer cases.

Table 21: Statistical analysis of V5-V4.51 radiative temperature differences (in Kelvin) in semi-transparent icy single-layer and multi-layer *upper levels*. April 2010.

	Night		Day	
	Mean	Standard deviation	Mean	Standard deviation
Single-layer	0.06	0.84	0.21	0.65
Multi-layer	0.39	2.5	0.57	2.7

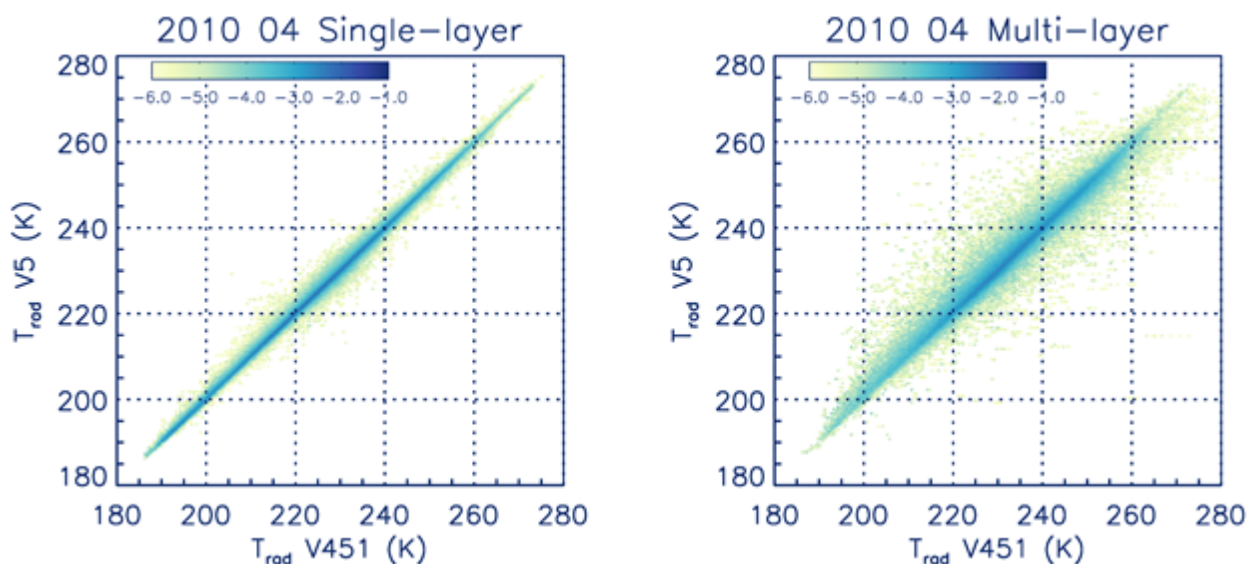


Figure 1: Comparison of V5 (Y-axis) and V4.51 (X-axis) radiative temperatures of upper levels composed of semi-transparent ice clouds for single-layer (left) and multi-layer (right) upper levels. The colors indicate the normalized number of samples in logarithm

Radiative height and pressure of the *upper level*

Radiative height and pressure corresponding to the radiative temperature of the *upper level* are now reported.

Cloud optical depth and estimated uncertainty

The V5 track product now includes cloud visible optical depth as retrieved by IIR when the *upper level* includes only ice clouds or only water clouds. For ice clouds, cloud optical depth is derived from effective emissivity at 10.6 and 12.05 μm using equation 11b in [Garnier et al. \(2021a\)](#). For water clouds, cloud optical depth varies with retrieved effective diameter (see equations 12 and 13a-b in [Garnier et al., 2021a](#)) and could be retrieved by the user from liquid water path and absorption optical depth at 12.05 μm . Cloud optical depth is provided in V5 for more clarity, and the estimated uncertainty is now available.

Suite of new “cirrus” retrievals in transparent ice clouds and estimated uncertainties

This V5 data release includes a new series of retrievals when the *upper level* is composed of semi-transparent ice clouds (new parameter names starting with “Cirrus”).

“Cirrus” optical and microphysical properties are retrieved using new analytical functions relating the $\beta_{\text{eff}12/10}$ microphysical index and various microphysical quantities derived from in situ measurements at tropical and mid-latitudes performed during the TC4, ATTREX, POSIDON, and SPARTICUS field experiments. These retrievals are detailed in [Mitchell et al. \(2025\)](#) where the analytical functions are shown in Table 3 and the strategy to combine them as a function of latitude and radiative temperature is summarized in Table 5.

The algorithm uses CALIOP in-cloud temperature and extinction profiles to estimate the equivalent layer thickness seen by IIR, which represents 30 to 90 % of the layer geometrical thickness (see section 6.1 in [Garnier et al., 2021a](#) and section 2.2.5 in [Mitchell et al., 2025](#)). This IIR equivalent thickness is used to retrieve the layer “vertically resolved” quantities, namely layer ice number concentration, layer extinction, and layer ice water content.

Both cirrus optical depth (Cirrus_Optical_Depth) and standard optical depth (Cloud_Optical_Depth) are derived using relationships between effective absorption efficiency at 12 μm ($Q_{\text{abs,eff}}(12 \mu\text{m})$) and $\beta_{\text{eff}12/10}$ microphysical index. For standard optical depth (COD), the retrieval equation is $\text{COD} = \tau_{a,10} + \tau_{a,12}$ where $\tau_{a,10}$ and $\tau_{a,12}$ are the effective absorption depths at 10.6 μm and 12.05 μm , respectively. This yields $1/Q_{\text{abs,eff}}(12 \mu\text{m}) = 0.5 \times (1 + 1/\beta_{\text{eff}12/10})$ when taking visible extinction = 2 as also assumed for the cirrus retrievals.

Figure 2 compares the standard and cirrus optical depth retrievals for the month of April 2010. The [standard – cirrus] relative optical depth difference is 9 % on average with a standard deviation of 13 %.

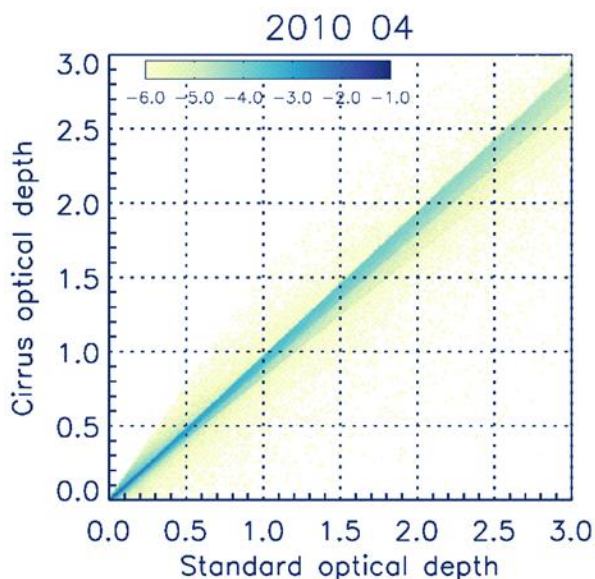


Figure 2: Comparison of cirrus (Y-axis) and standard (X-axis) optical depths of upper levels composed of semi-transparent ice clouds. The colors indicate the normalized number of samples in logarithm scale. April 2010.

Cirrus effective diameter (D_e) (Cirrus_Effective_Diameter) differs from standard D_e (Effective_Particle_Size) whose retrieval is based on various look-up tables assuming gamma particle size distributions and where both $\beta_{\text{eff}12/10}$ and $\beta_{\text{eff}12/08}$ microphysical indices are used to select the ice crystal model and ultimately produce D_e ([Garnier et al., 2021a](#)). Figure 3 shows cirrus D_e vs. standard D_e for single-layer columns over oceans where the particle shape index confidence parameter indicates confident standard retrievals. The horizontal lines at cirrus $D_e = 77.5$, 136.5 and 129.5 μm correspond to samples having $\beta_{\text{eff}12/10}$ smaller than the sensitivity limits of each of the 3 cirrus formulations below which D_e cannot be retrieved and is set to this maximum value. They correspond to standard D_e primarily between 60 and 120 μm .

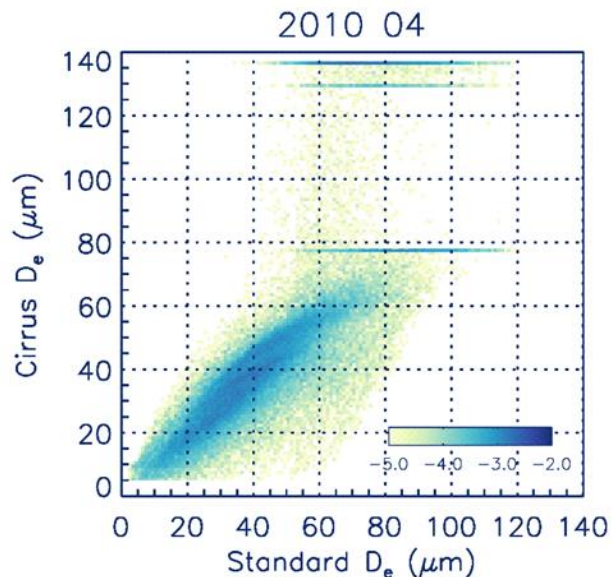


Figure 3: Comparison of cirrus (Y-axis) and standard (X-axis) effective diameters for single-layer semi-transparent ice columns over oceans and confident standard retrievals. The colors indicate the normalized number of samples in logarithm scale. April 2010.

Update Format of CALIPSO HDF Files

The V5.00 IIR Level 2 data products are distributed as Hierarchical Data Format Version 4 (HDF4) files, consistent with the EOS requirement in effect when CALIPSO launched in 2006. Since launch, there have been substantial technological advances in data discoverability and access resources. To make this data more readily accessible to the scientific community beyond the life of the mission and take advantage of newer data access capabilities, several modifications were made to the look and format of the WFC HDF files. These include:

- Update all units to conform to [NetCDF Climate and Forecast \(CF\)](#) metadata conventions.
- Verify all dimensions are named, to allow HDF to NCDF conversions using commercial off the shelf (COTS) tools that currently exist.
- Create/expand attributes and comments for all SDSs to make the data products more self-documenting.

Data Quality Statement for the release of the CALIPSO IIR Level 2 Product Version 4.51

The V4 IIR Level 2 algorithm, described in details in Garnier et al. ([2021a](#), [2021b](#)), takes full advantage of the co-located characterization of the atmosphere provided by CALIOP. The same V4 algorithm was used to generate these new V4.51 data products and the previous V4.2 data products. In V4.51, the V4 algorithm is applied to suitable types of scenes classified using the V4.51 CALIOP 5-km Cloud and Aerosol layer products, whereas the previous V4.2 data products were derived from the previous V4.2x CALIOP data products. The retrievals are applied to the so-called *upper level* which includes either one single semi-transparent or opaque layer, or several semi-transparent layers.

Data Quality Statement for the release of the CALIPSO IIR Level 2 Product Version 4.21

A minor version bump (+0.01) has been applied to all CALIPSO data products due to a required upgrade to the operating system on the CALIPSO production cluster. All algorithms were re-compiled to process in this new environment with no change to the underlying science algorithms or inputs.

Data Quality Statement for the release of the CALIPSO IIR Level 2 Product Version 4.20

The IIR Level 2 algorithm, described in details in Garnier et al. (2012, 2013), takes full advantage of the co-located characterization of the atmosphere provided by CALIOP. It is applied to suitable types of scenes classified using the V4.20 CALIOP 5-km Cloud and Aerosol layer products. The retrievals are applied to the so-called *upper level* cloud which includes either one single semi-transparent or opaque layer, or several semi-transparent layers.

Effective emissivity retrievals require i) a correction for the contribution from the “background” and ii) the determination of the radiative temperature of the *upper level* cloud. When the lowermost of at least two individual cloud layers in the column is opaque to CALIOP, the background reference is from this opaque layer, which is called *lower level*. Otherwise, the background reference is from the Earth surface in clear air conditions. Both in the older V3 and in V4, the first step into the computation of the radiative temperature is to determine the centroid altitude of the *upper level* cloud.

As in V3, ice cloud effective diameter (D_e) retrievals use the concept of microphysical index (β_{eff}) applied to the IIR pairs of channels (12.05, 10.6) and (12.05, 8.65), with $\beta_{\text{eff}12/10}$ and $\beta_{\text{eff}12/08}$ defined as the 12.05-to-10.6 and 12.05-to-08.65 ratios of the effective absorption optical depths, respectively. The microphysical indices are interpreted in terms of D_e by using Look-Up Tables (LUTs) built for several models. The ice water path is then determined from calculated effective emissivities and D_e .

The most significant changes in the V4 algorithm with respect to V3 include:

- A refined scene classification
- An updated radiative transfer model analysis for clear air reference with new surface emissivity values and corrected land surface temperature
- A revised centroid altitude in multi-layer cases
- Refined radiative temperature estimates in ice clouds
- Updated and extended microphysical retrievals in ice clouds
- Addition of microphysical retrievals in liquid water clouds
- Revised uncertainty estimates

Refined Scene Classification

Was_Cleared_Flag_1km

In V4, a new “Was_Cleared_Flag_1km” parameter reports the number of clouds seen by the 1-km IIR pixel that were detected by CALIOP at single shot resolution and that were cleared from the CALIOP 5-km layer products. These clouds have a top altitude < 4 km. In V3, these single-shot cleared clouds were not reported in the CALIOP 5-km layer products and they were ignored by the IIR algorithm.

In V4, the cloud-free (clear sky or aerosol only) scenes must have Was_Cleared_Flag_1km = 0. When Was_Cleared_Flag_1km ≠ 0, these scenes, which were thought to be cloud-free in V3, are assigned new types of scenes in V4.

For effective emissivity retrievals, the background radiance is computed regardless of Was_Cleared_Flag_1km. Unless the bias in the background radiance due to the cleared clouds can be estimated a posteriori and can be deemed acceptable, it is recommended to ensure that Was_Cleared_Flag_1km = 0 for detailed analyses of retrievals in optically thin clouds.

Absorbing Aerosols

For the scenes that fall into the “clouds” category, the semi-transparent aerosol layers, if any, are ignored when computing the cloud effective emissivity. In V4, we require that the “clouds” scenes that contain only one or two

semi-transparent cloud layers do not contain high (typically stratospheric) aerosol layers, because these high aerosol layers could absorb in the IIR channels.

In addition, the presence of potentially absorbing aerosol layers (i.e. tropospheric dust or stratospheric aerosols) is now reported in a new `Dust_Stratospheric_Aerosol_Flag` and a new `Dust_Stratospheric_Aerosol_Flag_QA` so that the retrievals can be filtered using these flags.

Updated Radiative Transfer Model Analysis for Clear Air Reference

When no relevant neighboring observations can be found, the background reference is computed using a radiative transfer model, meteorological profiles and surface temperature from MERRA-2 re-analyses, and surface emissivity values.

Model

The radiative transfer model has been updated in V4 to better simulate absorption by water vapor.

Surface Category, Surface Emissivity, and Surface Temperature

In V3, the surface emissivity values in each IIR channel were theoretical static values assigned to each IGBP Surface Type. When the daily `Snow_Ice_Surface_type` indicated the presence of snow or sea ice, IGBP Surface Type was changed to IGBP = 15 (snow/ice).

In V4, the characterization of the surface has been refined, and is reported in a new “TGeotype” parameter. TGeotype is assigned using IGBP Surface Type and the co-located `Surface_532_Integrated_Depolarization_Ratio`, now reported in the V4 CALIOP products, and `Snow_Ice_Surface_type` if `Surface_532_Integrated_Depolarization_Ratio` is not available. `Surface_532_Integrated_Depolarization_Ratio` is also used to refine the land/water classification around coastlines. The TGeotype values fall into five main categories: water, water/sea ice transition, sea ice, snow, and snow-free land.

Surface emissivity values used in V4 have been determined empirically from the analysis of two years of IIR data in clear sky conditions. The V4 algorithm continues to use static values for the water, water/sea ice transition, sea ice, and snow categories. For the snow-free land category, the V3 static values per IGBP type at 08.65 μm and 10.6 μm are replaced with monthly daytime and nighttime maps (resolution: latitude x longitude = $1^\circ \times 2^\circ$), while a constant value (0.975) is taken at 12.05 μm . In case of snow-free land, the surface temperature is the initial MERRA 2 surface temperature further corrected using monthly daytime and nighttime correction maps that were derived using the 12.05 μm reference channel by reconciling calculations and IIR observations.

Summary of Clear Air Reference Changes from V3 to V4

The changes described above improve the accuracy of effective emissivity and microphysical retrievals in optically thin layers when the clear air background radiance is derived from the model. Subsequently, retrievals derived from observed and computed background radiances are more consistent in V4 than in V3.

Over oceans, the change from V3 to V4 is for the most part the reduction of systematic effective emissivity biases at 08.65 μm , which improves the reliability of effective diameter retrievals. Even though less accurate than over oceans, retrievals over land are improved in V4, in particular in desertic areas and in polar regions.

Revised Centroid Altitude in Multi-layer Cases

Because of an error in the V3 algorithm, the centroid altitude of multi-layer systems could be too low by up to 3 km in V3. This has been fixed in V4.

Refined Radiative Temperature Estimates in Ice Clouds

In V3, the radiative temperature was set to the temperature at the lidar centroid altitude for any cloud or aerosol system. The approach is the same in V4, except when all the layers are classified as ice by the V4 CALIOP ice/water phase algorithm. In the latter case, the initial centroid temperature estimate (which was used in V3) has been shown to be too cold ([Garnier et al., 2015](#)). It is now refined in V4 using parameterized correction functions. Blackbody brightness temperatures derived from both the centroid temperature and the V4 radiative temperature are reported in the V4 product.

The correction applied in V4 has a negligible impact on effective emissivity values smaller than about 0.3. The largest impact is for opaque clouds, the correction being more efficient for nighttime than for daytime data. For instance, for oceanic opaque ice clouds in January 2008, nighttime and daytime distributions of effective emissivity at 12.05 μm peak respectively at 0.99 and 0.97 in V4, compared to 0.94 in V3.

Updated Microphysical Retrievals in Ice Clouds

Optical Properties

The three ice crystal models used in V3 have been replaced with two ice crystal models in V4, namely severely rough “single hexagonal column” and “8-element column aggregate” elaborated from new ice properties ([Yang et al., 2013](#); [Bi and Yang, 2017](#)). In addition, a gamma particle size distribution with effective variance equal to 0.1 is taken in V4, whereas there was no size distribution in V3. As a result of these changes, D_e is increased from V3 to V4.

Four independent sets of D_e derived from a second approach are also reported in V4. This approach uses analytical functions relating $\beta_{\text{eff}12/10}$ and D_e as derived from in situ measurements at tropical and mid-latitudes performed during the TC4 and SPARTICUS field experiments ([Mitchell et al., 2018](#)).

Ice Water Path

For ice clouds, Ice Water Path is estimated from D_e and visible extinction optical depth (τ_{vis}) derived from calculated effective emissivities. In V3, τ_{vis} was approximated to $2\tau_{a,12}$, where $\tau_{a,12}$ is the IIR affective absorption optical depth at 12.05 μm . In V4, τ_{vis} is approximated to $\tau_{a,12} + \tau_{a,10}$, where $\tau_{a,10}$ is the IIR affective absorption optical depth at 10.6 μm . The V4 approximate reduces the dependence on D_e and improves the τ_{vis} estimate by up 10 % for $D_e > 20 \mu\text{m}$.

Addition of Microphysical Retrievals in Liquid Water Clouds

Unlike in V3, microphysical retrievals in liquid water clouds are provided in V4.

For D_e retrievals, the LUTs are computed using the Mie theory with refractive indices from [Hale and Query \(1973\)](#) and again using a gamma particle size distribution (PSD) with effective variance equal to 0.1. No temperature dependence of infrared absorption is included.

Liquid Water Path is estimated from D_e , $\tau_{a,12}$, and $Q_{a,12}(D_e)$, where the latter is the effective absorption efficiency at 12.05 μm , whose variation with $D_e \leq 20 \mu\text{m}$ is represented using a fourth-degree polynomial. In agreement with [Pinnick et al. \(1979\)](#), $Q_{a,12}$ increases quasi-linearly with $D_e < 10 \mu\text{m}$ up to about 1, and then increases slowly up to 1.15 as D_e increases from 10 to 20 μm .

Revised Uncertainty Estimates

For each IIR channel, the estimated uncertainty in the effective emissivity is composed of three terms associated to

- an error dT_m in the measured brightness temperature,
- an error dT_{BG} in the background reference brightness temperature,
- an error dT_{BB} in the blackbody temperature.

In V3, the reported uncertainties were computed using $dT_m = dT_{BG} = dT_{BB} = 1$ K. Table 22 describes the temperature errors used in V4.

Table 22: Contributions to the Estimated Effective Emissivity Uncertainties Based on Surface

	Water Surface	Non-Water Surface
$dT_m(K)$	0.3	0.3
$dT_{BG}(K)$	1	3
$dT_{BB}(K)$	2	2

In V4, the three terms used to compute the estimated uncertainty in the effective emissivity are reported.

Effective Diameter Uncertainty

The approach chosen to report the estimated uncertainty in D_e has been changed in V4. In V4, it is simply inferred from the estimated uncertainty in the microphysical indices and from the LUT used for the retrievals.

Ice or Liquid Water Path Uncertainty

Unlike in V3, an estimated uncertainty in the ice or liquid water path is reported in V4. It is computed from the estimated uncertainty in D_e and in the effective absorption optical depth(s).

Data Quality Statement for the release of the CALIPSO IIR Level 2 Product Version 3.46

A minor version bump (+0.01) has been applied to all CALIPSO data products due to a required upgrade to the operating system on the CALIPSO production cluster. All algorithms were re-compiled to process in this new environment with no change to the underlying science algorithms or inputs.

Data Quality Statement for the release of the CALIPSO IIR Level 2 Product Version 3.45

All CALIPSO science data executables were migrated to a new production cluster. Because of the need to make minor algorithm changes and recompile, the version number of the IIR Level 2 data products has changed from V3.40 to V3.45. All other data products successfully transferred without the need to recompile and retain their existing versioning.

Data Quality Statement for the release of the CALIPSO IIR Level 2 Product Version 3.40

Version 3.40 data products reflect a transition of the Global Modeling and Assimilation Office (GMAO) Forward Processing – Instrument Teams (FP-IT) meteorological data version from 5.9.1 to 5.12.4.

Data Quality Statement for the release of the CALIPSO IIR Level 2 Product Version 3.30

Version 3.30 data products incorporate the updated GMAO Forward Processing - Instrument Teams (FP-IT) meteorological data, and the enhanced Air Force Weather Authority (AFWA) Snow and Ice Data Set as ancillary inputs to the production of these data sets, beginning with data date March 1, 2013.

Impacts on CALIOP data products, of which IIR Level 2 use as input, caused by the transition to GEOS-5 FP-IT are predicted to be minimal, based on a comparison of CALIOP Version 3.02 against CALIOP Version 3.30.

IIR Level 2 algorithm uses ancillary surface and atmospheric data to compute background and blackbody radiances before retrieving effective emissivity and optical depth.

In case of cirrus clouds over ocean, absorption optical depth derived from computed background radiances is predicted to change by less than 0.01 on average between 60S and 60N, and to be more accurate in V3.30. These predictions are inferred from distributions of brightness temperature (BT) differences between observations and computations in clear sky conditions over ocean for several ranges of latitude in August 2013 (V3.30), which have been compared to distributions for the months of August 2012 and 2010 (V3.02 and V3.01, respectively). The mean BT differences are reduced by 0.1 to 0.3 Kelvin in absolute value in V3.30, with similar standard deviations (1.2 and 1.9 Kelvin). At high latitude, a more accurate identification of the IIR pixels not impacted by snow or ice results into smaller standard deviations in V3.30. No significant change of the computed blackbody radiances has been identified for opaque ice clouds for the month of August 2013.

In case of cirrus clouds overlying a low opaque cloud, changes in absorption optical depth derived from computed background radiances are predicted from distributions of differences between observations and computations for low opaque clouds. The median BT differences are improved by 0.4 to 1.2 Kelvin in August 2013 (V3.30) compared to August 2010 and 2012, corresponding to changes of the order of 0.01 to 0.03 in absorption optical depth.

Data Quality Statement for the release of the CALIPSO IIR Level 2 Product Version 3.02

Version 3.02 reflects a change in the data products due to a required upgrade to the operating system on the CALIPSO production cluster. All algorithms were re-compiled to process in this new environment with no change to the underlying science algorithms or inputs

Data Quality Statement for the release of the CALIPSO IIR Level 2 Product Version 3.01

Version 3.01 includes microphysical parameters which were not available in Version 2: effective particle size and uncertainty, particle shape and confidence, and ice-water path. The optical depth derived from the effective emissivity at 12.05 μm has been added.

Version 3.01 IIR scene classification algorithm has been updated with respect to Version 2 (cf Type of Scene, IIR/Lidar track product). Also, Version 3.01 IIR products use Version 3.01 CALIOP Level 2 products (instead of Version 2 for the previous release). Overall, changes in the IIR scene classification are significant in Version 3.01 compared to Version 2.

Data Quality Statement for the release of the CALIPSO IIR Level 2 Product Version 2.20

N/A

Data Quality Statement for the release of the CALIPSO IIR Level 2 Product Version 2.01

N/A

References

- Bi, L. and P. Yang, 2017: Improved ice particle optical property simulations in the ultraviolet to far-infrared regime, *J. Quant. Spectrosc. Radiat. Transfer*, **189**, 228–237, <https://doi.org/10.1016/j.jqsrt.2016.12.007>.
- Garnier, A., J. Pelon, M. A. Vaughan, D. M. Winker, C. R. Trepte, and P. Dubuisson, 2015: Lidar multiple scattering factors inferred from CALIPSO lidar and IIR retrievals of semi-transparent cirrus cloud optical depths over oceans, *Atmos. Meas. Tech.*, **8**, 2759–2774, <https://doi.org/10.5194/amt-8-2759-2015>.
- Garnier, A., T. Trémas, J. Pelon, K.-P. Lee, D. Nobileau, L. Gross-Colzy, N. Pascal, P. Ferrage, and N. A. Scott, 2018: CALIPSO IIR Version 2 Level 1b calibrated radiances: analysis and reduction of residual biases in the Northern Hemisphere, *Atmos. Meas. Tech.*, **11**, 2485–2500, <https://doi.org/10.5194/amt-11-2485-2018>.
- Hale, G. M. and M. R. Query, 1973: Optical constants of water in the 200 nm to 200 μm wavelength region, *Appl. Opt.*, **12**, 555–563, <https://doi.org/10.1364/AO.12.000555>.
- Parol, F., J. C. Buriez, G. Brogniez, and Y. Fouquart, 1991: Information content of AVHRR channels 4 and 5 with respect to the effective radius of cirrus cloud particles, *J. Appl. Meteor.*, **30**, 973–984, <https://doi.org/10.1175/1520-0450-30.7.973>.
- Pinnick, R. G., S. G. Jennings, P. Chylek, and H. J. Auvermann, 1979: Verification of a linear relation between IR extinction, absorption and liquid water content of fogs, *J. Atmos. Sci.*, **36**, 1577–1586, [https://doi.org/10.1175/1520-0469\(1979\)036<1577:VOALRB>2.0.CO;2](https://doi.org/10.1175/1520-0469(1979)036<1577:VOALRB>2.0.CO;2).
- Tackett, J. L., R. A. Ryan, A. E. Garnier, J. Kar, B. Getzewich, X. Cai, M. A. Vaughan, C. R. Trepte, R. Verhappen, D. M. Winker, and K.-P. A. Lee, 2025: Mitigating impacts of low energy laser pulses on CALIOP data products, *Atmos. Meas. Tech.*, **18**, 6211–6231, <https://doi.org/10.5194/amt-18-6211-2025>.
- Yang, P., H. Wei, H. L. Huang, B. A. Baum, Y. X. Hu, G. W. Kattawar, M. I. Mishchenko, and Q. Fu, 2005: Scattering and absorption property database for non-spherical ice particles in the near-through far-infrared spectral region, *Appl. Opt.*, **44**, 5512–5523, <https://doi.org/10.1364/AO.44.005512>.
- Yang, P., L. Bi, B. A. Baum, K.-N. Liou, G. W. Kattawar, M. I. Mishchenko, and B. Cole, 2013: Spectrally consistent scattering, absorption, and polarization properties of atmospheric ice crystals at wavelengths from 0.2 μm to 100 μm , *J. Atmos. Sci.*, **70**, 330–347, <https://doi.org/10.1175/JAS-D-12-039.1>.